DHA-induced stress response in human colon cancer cells - focus on oxidative stress and autophagy

Kristine Pettersen[a,b,d,*], Vivi Talstad Monsen[a,*], Caroline Hild Hakvåg Pettersen[a], Hilde Bremseth Overland[a,c], Grete Pettersen[a], Helle Samdal[a], Almaz Nigatu Tesfahun[a], Anne Gøril Lundemo[a], Geir Bjørkøy[b,d,**] and Svanhild Schønberg[a,**,†]

a) Department of Laboratory Medicine, Children's and Women's Health, Faculty of Medicine, Norwegian University of Science and Technology, 7006 Trondheim, Norway

b) Department of Technology, Erling Skjalgssons gt. 1, University College of Sør-Trøndelag, 7006 Trondheim, Norway

c) Central Norway Regional Health Authority, 7055 Stjørdal, Norway

d) Centre of Molecular Inflammation Research, Department of Cancer Research and Molecular Medicine, Norwegian University of Science and Technology, 7491 Trondheim, Norway

Running title: Role of NFE2L2 and autophagy in response to DHA

*) These authors have contributed equally to this work

**) Shared senior authorship

†) corresponding author:

Svanhild A. Schønberg

Dept. of Laboratory Medicine, Children's and Women's Health,

Faculty of Medicine, NTNU

7006 Trondheim, Norway

Phone: +47 95788616

E-mail address: svanhild.schonberg@ntnu.no

ABSTRACT

Polyunsaturated fatty acids (PUFAs) are important constituents of the diet and health benefits of omega-3/n-3 PUFAs, especially eicosapentaenoic acid (EPA, 20:5 n-3) and docosahexaenoic acid (DHA, 22:6 n-3) have been well documented in relation to several diseases. Increasing evidence suggests that n-3 PUFAs may have anticancer activity and improve the effect of conventional cancer therapy. The mechanisms behind these effects are still unclear and need to be elucidated.

We have examined the DHA-induced stress response in two human colon cancer cell lines, SW620 and Caco-2. SW620 cells are growth-inhibited at early time points by DHA, while the growth of Caco-2 cells almost remains unaffected by the same treatment. Gene expression analysis of SW620 cells treated with DHA revealed changes at early time points; transcripts involved in oxidative stress and autophagy were among the first to be differentially expressed. We find that oxidative stress is induced in both cells lines, although at different time points and to different extents. DHA induced nuclear translocation of the oxidative stress sensor NFE2L2 in both cell lines, indicating an induction of an anti-oxidative response. However, vitamin E did not counteract ROS-production or the translocation of NFE2L2 to the nucleus. Neither vitamin E nor the antioxidants butylated hydoxyanisole (BHA) and butylated hydoxytoluene (BHT) did affect the growth inhibition in SW620 cells after DHA-treatment. Also, siRNA-mediated down-regulation of NFE2L2 did not sensitize SW620 and Caco-2 cells to DHA. These results indicate that oxidative stress response is not the cause of DHA-induced cytotoxicity in SW620 cells.

Using biochemical and imaging based functional assays, we found a low basal level of autophagy and no increase in autophagic flux after adding DHA to the SW620 cells. However, Caco-2 cells displayed a higher level of autophagy, both in the absence and presence of DHA. Inhibition of autophagy by siRNA mediated knock down of ATG5 and

ATG7 sensitized both SW620 and Caco-2 cells to DHA. Stimulation of autophagy by rapamycin in SW620 and Caco-2 cells resulted in decreased DHA-sensitivity and inhibition of autophagy in Caco-2 cells by chloroquine resulted in increased DHA-sensitivity.

These results suggest that autophagy is important for the DHA sensitivity of colon cancer cells and imply possible therapeutic effects of this fatty acid against cancer cells with low autophagy.

Keywords: n-3 PUFA, DHA, oxidative stress, autophagy, NFE2L2, colon cancer

Introduction

Several epidemiological studies have pointed to a positive correlation between dietary fish intake and the reduced risk of developing age related disorders such as circulatory disturbances, neurodegenerative diseases, and different types of cancer [1-3]. The disease preventive effects of increased fish intake have been associated with the content of omega-3 (n-3) polyunsaturated fatty acids (PUFAs) present in marine species [4]. Case-control studies have suggested an inverse correlation between dietary fish intake and colorectal cancer [5, 6]. N-3 PUFAs have been shown to inhibit growth of human cancer cells in culture and when grafted in mice [7, 8]. Several mechanisms have been proposed to explain the anticancer activity mediated by n-3 PUFAs like increased oxidative stress, lipid peroxidation, modulation of cyclooxygenase activity and changes in membrane phospholipid composition and receptor function [9-11]. However, why some cancer cells die and others survive when exposed to n-3 PUFAs is still poorly defined.

We have previously shown that docosahexaenoic acid (DHA, 22:6 n-3) induces endoplasmic reticulum (ER) stress, unfolded protein response (UPR) and growth arrest in several human cancer cell lines [12-14]. Increased protein levels of PKR-like ER kinase (PERK)-mediated phosphorylation of eukaryotic translation initiation factor 2alpha (eIF2α), indicative of ER stress, were found at early time points [14]. The main functions of the ER are protein synthesis and folding, maintenance of calcium homeostasis and lipid synthesis. Interference with any of these processes may lead to ER-stress and activation of UPR in order to restore cellular homeostasis. The activation of UPR is followed by attenuation of protein translation and activating transcription factor 4 (ATF4) mediated up-regulation of genes to ensure cell survival or to mediate cell death when stress is too severe.

Recently, it has become clear that induction of ER stress as well as several other forms of cellular stress like nutrient deprivation, reactive oxygen species (ROS), DNA damage, protein

aggregates and damaged organelles may lead to the induction of autophagy as reviewed in [15]. Macroautophagy (hereafter referred to as autophagy) is a catabolic process that removes damaged cellular components to maintain cellular integrity and stability [16]. During the autophagic process, cytoplasmic proteins and organelles are sequestered by a growing double membrane that forms an autophagosomal vesicle, and the content is degraded after fusion with a lysosome. A basal activity of autophagy is needed to maintain normal cellular homeostasis, and the level of activity may be increased in response to different kinds of stresses [17, 18]. Dysregulation of this process is linked to different conditions like neurodegeneration, aging, cancer, and infectious-, cardiovascular- and metabolic diseases. In cancer, autophagy has dual roles by acting both as a tumor suppressor preventing initiation of tumorigenesis, but also by assisting cancer cells in coping with stressful conditions thereby promoting cancer cell growth [19]. Autophagy is a highly evolutionary conserved process that is regulated by autophagy-related genes (*ATGs*) [20]. The ATG 1/Unc-51-like kinase 1/2 ULK1/2 kinase is considered a principal regulator of autophagy [21]. The ULK1/2 kinase activity and its ability to stimulate autophagy is negatively regulated by the mammalian target of rapamycin complex 1, mTORC1 [22]. When activated, mTOR inhibits autophagy by phosphorylation of ULK1 [23]. The tumor suppressors 5’ AMP-activated protein kinase (AMPK), phosphatase and tensin homolog (PTEN), liver kinase B1 (LKB1) and tuberous sclerosis 1/2 (TSC1/2) positively regulate autophagy both by inhibiting mTOR and by activating the ULK1/2 activity directly [21]. ATF4 also regulates mTOR activity negatively via transcriptional up-regulation of DNA-damage-inducible transcript 4 (REDD1) [24]. During ER stress, the PERK-eIF2α-ATF4 branch of UPR is required for increased expression of REDD1. ER stress may also lead to the production of ROS and vice versa; it is however not clear whether oxidative stress is involved in autophagy mediated by ER stress.

The redox-sensitive transcription factor nuclear factor erythroid-2-related factor-2 (NFE2L2/Nrf-2) regulates the expression of genes involved in the endogenous antioxidant response [25]. Under unstressed conditions, NFE2L2 is distributed in the cytoplasm in association with kelch like-ECH-associated protein 1 (KEAP1), a protein essential for the regulation of NFE2L2 activity through degradation via the ubiquitin-proteasome system [26]. When stress is induced, NFE2L2 is phosphorylated and dissociates from KEAP1 and translocates to the nucleus where it activates target genes involved in the antioxidant defense or phase II detoxification through interaction with the antioxidant response element (ARE) [27]. NFE2L2 has also been shown to be a direct substrate for the PERK kinase activity. Upon ER stress, PERK phosphorylates NFE2L2 to promote dissociation from KEAP1 and translocation to the nucleus [28]. The sequestosome 1 protein (SQSTM1/p62) is a scaffold protein involved in clearance of ubiquitinated protein aggregates and organelles through selective autophagy [29, 30]. The promoter of SQSTM1 contains an ARE-element and transcription of SQSTM1 is thus regulated by NFE2L2 [31]. SQSTM1 has also been shown to interact with KEAP1 at the NFE2L2 binding site, leading to NFE2L2 release and translocation to the nucleus thereby contributing to a positive feedback regulation of self-transcription [32].

The signaling pathways of ER stress, oxidative stress and autophagy are complex and seem to be interrelated. We have previously shown by gene expression profiling that treating the human colon cancer cell line SW620 with the n-3 PUFA DHA increases the level of transcripts involved in ER stress and NFE2L2 target transcripts like heme oxygenase 1 (HMOX1), glutamate-cysteine ligase modifier (GCLM), thioredoxin reductase 1 (TXNRD1) and SQSTM1/SQSTM1 [14]. In this study we explore whether oxidative stress and/or autophagy could be involved in modulating the cytotoxic effect of DHA in human colon cancer cell lines.

We here report that oxidative stress- and autophagy-related transcripts are among the primary response genes to DHA in SW620 colon cancer cells. Vitamin E did not counteract DHA-induced ROS, did not interfere with nuclear translocation of NFE2L2 and did not restore cell growth in SW620 cells. SiRNA-mediated down-regulation of NFE2L2 did not sensitize Caco-2 cells to DHA. These results indicate that oxidative stress is not the cause of DHA-induced cytotoxicity in SW620 cells. Even though several autophagy related genes are induced in the sensitive SW620 cells in response to DHA, no evident activation of the autophagy process could be observed in these cancer cells. Inhibition of autophagy by siRNA mediated knock down of ATG5 and ATG7 sensitized both SW620 and Caco-2 cells to DHA while stimulating autophagy in both cell lines by inhibiting mTOR resulted in decreased DHA sensitivity.

Our results indicate that the basal level of autophagy is important for surviving the cellular stress induced by DHA and suggest that colon cancer cells with low basal autophagy are more sensitive to stress and may be targeted by DHA.

Materials and Methods

Cell cultures and reagents

SW620 and Caco-2 cells were obtained from American Type Culture Collection (ATCC) (Rockville, MD). SW620 cells were cultured in Leibovitz's L-15 medium (#BE-12-700, Lonza, Basel, Switzerland), supplemented with L-glutamine (#17-605E, Lonza, 2 mM), Fetal Bovine Serum (FBS, 10270, Gibco, 10%) and Gentamicin (#15710049, Gibco, 0.05 mg/ml). Caco-2 cells were cultured in Eagle medium (#M5650, Sigma-Aldrich) supplemented with L-glutamine (#17-605E/ Lonza, 2 mM), Sodium pyruvate (#P5280, Sigma-Aldrich, 1%), Gentamicin (0.05 mg/ml), and FBS (20%). Cells were maintained in a humidified atmosphere of 5% CO_2; 95% air at 37°C.

4,7,10,13,16,19-docosahexaenoic acid (DHA) and 9-octadecanoic acid (OA) were obtained from Cayman Chemical (Ann Arbor, MI) as solutions in ethanol. Vitamin E (±-α-tocopherol, T3251), Butylated hydroxyanisole (BHA, B1253), Butylated hydroxytoluene (BHT, B1378), Rapamycin (R8781), Bafilomycin A1 (BafA1, B1793), Chloroquine (Chl, C6628) and Hanks' Balanced Salt Solution (HBSS, #H8264) were obtained from Sigma-Aldrich (St. Louis, MO).

The following primary antibodies were used: Specific to SQSTM1 (#GP-62-C, Progen Biotechnik; NFE2L2 (#sc-13032, H-300, Santa Cruz Biotechnology, Inc. and #12721, D1Z9C, Cell Signaling Technologies); LC3B-II (#3868, D11, Cell Signaling Technologies); HMOX1 (#ADI-OSA-110, Stressgen); BAG3 (#ab47124, Abcam); HSPA1A (#SPA-810, Stressgen), ACTB (#ab6276, AC-15, Abcam); TUBB (#ab6046, Abcam); COX IV (#ab33985, Abcam and #926-42214, Li-cor Biotechnology, Inc), KEAP1 (#sc-15246, E20, Santa Cruz Biotechnology, Inc), TRIB3 (#HPA015272, Sigma Aldrich). All secondary antibodies were from Molecular Probes (Alexa conjungates) or Li-Cor Biotechnology (NIR dye conjungates)

Fatty acid supplementation and survival assays

Stock solutions of fatty acids in ethanol were stored at -20°C and further diluted in complete growth medium with FBS before experiments, such that the final concentration of ethanol was < 0.025% (v⁄v). DHA/OA/BafA1-treatments were initiated 24 h after cell seeding. MTT-assay was performed as previously described [12].

Cell proliferation was also monitored in real time using the xCELLigence RTCA DP instrument (ACEA Biosciences Inc) according to the supplier's recommendations. Where indicated, the cells were pretreated with 50 nM rapamycin for 30 min before adding fresh medium containing vehicle or DHA. For inhibition of autophagy, chloroquine (10 μM) was

added alone or in combination with DHA (70 μM). For starvation, total L-15 medium was diluted with 50% HBSS.

Gene expression profiling

SW620 cells were treated with vehicle (ethanol) or 70 μM DHA for 30 min, 1, 3, 6, 24 and 48 h before RNA isolation. Expression profiling was performed in triplicates at all time points, except for 1 h, where one control array was excluded. The statistical analysis was based on summary expression measures using the raw data (CEL) files performed by the robust multiarray average method as previously described [14, 33]. The statistical analysis was performed in R (http://www.r-project.org), using packages Limma and Affy from Bioconductor. Differentially expressed genes were selected based on a threshold of 0.05 on the adjusted *P* values. All data have been submitted to ArrayExpress with the accession numbers E-MEXP-2010 (30 min, 1, 3, 6 h) and E-MEXP-1014 (12, 24, 48 h).

siRNA mediated knock down and transient transfection

For NFE2L2 down regulation, Caco-2 cells and SW620 cells were transfected using 10 to 20 nM and 50 nM siRNA (final concentrations), respectively and DharmaFECT transfection reagent 1 (Dharmacon) diluted in Optimem 1 Reduced Serum Medium (#31985-070, Gibco Life Technologies). Following 24 h, the cells were collected by trypsination and seeded for real-time cell monitoring, cell counting and immunoblot analysis. The following siRNA oligonucleotides were obtained from Dharmacon; non-targeting siRNA (D-001210-01); NFE2L2 siRNA (D-003755-02, target sequence: 5`-CCAAAGAGCAGUUCAAUGA); ATG5 (L-004374-00) and ATG7 (L-020112-00), SQSTM1 (J-010230-06-0020, target sequence 5`-GCAUUGAAGUUGAUAUCGA) and HMOX1 (D_006372-05-0050, target

sequence: 5'-GGCAGAGGGUGAUAGAAGA). Allstars negative control siRNA (#1027280) and Allstar HS Cell Death Control siRNA (#1027298) were obtained from Qiagen.

The double tag mCherry-EGFP [30] was transfected into the cells using X-treme GENE HP DNA Transfection Reagent (Roche) following the supplier's recommendations. After transfection, cells were seeded in wells with cover-glass bottom, left for 24 h before adding vehicle or DHA for 16 h. Cells were fixated using 4% para-formaldehyde in PBS (pH 7.2) for 10 min and stored in PBS until confocal microscope imaging. The number of punctuated green and red structures per cell was determined in more than 100 cells per condition per experiment.

Detection of ROS and lipid peroxidation

ROS production was determined using the Image-iT ™ LIVE Green Reactive Oxygen Species Detection Kit (DCF, Molecular Probes) and a BD FACS Canto flow cytometer (BD Biosciences) in SW620 and Caco-2 cells. As a positive control, 100 µM *tert*-butyl hydroperoxide (TBHP) was added 80 min before intracellular ROS was determined. Mitochondrial superoxide production was determined using 5 µM MitoSOX^{TM} Red (Molecular Probes) mitochondrial superoxide indicator.

Lipid peroxidation in Caco-2 cells was measured as the secondary lipid peroxidation product malondialdehyde (MDA) using the OxiSelectTM TBARS Assay Kit (Cell Biolabs, INC). Caco-2 cells were treated with vehicle , DHA (70 µM), vitamin E (50 µM) or co-treated with DHA (70 µM) and vitamin E (50 µM) for 72 h before scraping in ice cold PBS and frozen in aliquots of 20×10^6 cells/ml. MDA reacts with thiobarbituric acid (TBA) resulting in thiobarbituric acid reactive substances (TBARS) that are measured colorimetically.

Cellular localization of autophagy biomarkers and NFE2L2

Subcellular localization of SQSTM1, NFE2L2 and LC3B was determined by immunostaining and visualization by fluorescently labeled secondary antibodies. Immunostaining was imaged by an Axiovert200 microscope equipped with a 63 x 1.2W objective and the confocal module LSM510 META (Carl Zeiss). Images were processed using the LSM software (Carl Zeiss) and mounted using Canvas 11 (ACD Systems). Images are representative of more than 200 randomly selected cells in each condition and of two or more independent experiments. Cytoplasmic structures enriched for LC3 were quantified by using the histogram function in the LSM software. All images were taken with the same settings. Pixels positive for LC3B with an intensity of more than 100 RLU were counted and divided by the number of cells in the image (more than 100 cells per condition).

Autophagy determined by flow cytometry

Autophagic structures were determined using the CytoID autophagy detection kit following the suppliers' instructions (Enzo Life Sciences). Briefly, the cells were detached by trypsination and stained in a solution with Cyto-ID Detection Reagent covered from light for 30 minutes at room temperature with gentle rotation, and the fluorescent intensity per cell was determined using a flow cytometer.

Immunoblotting

Cells, transfected or non-transfected, untreated or treated with DHA and/or 100 nM BafA1, were harvested by trypsinization or scraped in ice cold PBS. Cells were lysed in either a buffer containing 1% NP40, 0.25% Triton-X100, 50 mM Tris-HCl (pH 8.0), 150 mM NaCl, 1 mM EDTA pH 8, Complete® protease inhibitor (PI, Roche), and phosphatase inhibitor cocktail I and III (Sigma-Aldrich), or an urea buffer containing 8M Urea, 0.5% (v/v) Triton X-100, 100 mM DTT, PI, and phosphatase inhibitor cocktail I and III. Total protein

concentration in the lysates was determined by Bio-Rad protein assay (Bio-Rad). Bound antibodies were imaged by near infrared fluorescence using appropriate fluorescent dye labeled secondary antibodies and an Odyssey NIR scanner (Li-Cor Biosciences). Images were processed using the Li-Cor Odyssey software and mounted using the Canvas 11 software (ACD Systems).

Results

DHA induces changes in expression of genes involved in oxidative stress, protein folding and autophagy at early time points

The effect of DHA on cell growth/cell index of the colon cancer cell lines SW620 and Caco-2 was determined by MTT assay and real time analysis (xCELLigence System), respectively (Fig. 1). The effect on cell growth/cell index measured by both systems corresponded well. We found that DHA reduced growth of SW620 cells in a time- and concentration-dependent manner, as measured by the MTT assay. Cell viability started to decline after approximately 24 h supplementation with DHA (70 µM) in SW620 cells; a 30% and 50% reduction in cell viability could be observed after 48 and 72 h, respectively. The cell growth/cell index of Caco-2 cells were almost unaffected by the same treatment. Supplementation of SW620 cells with the monounsaturated fatty acid oleic acid (OA) (18:1, n-9) did not result in any change in cell index relative to control cells. The relative differences in response to DHA were verified by conventional cell counting (data not shown). The rapid growth retardation after supplementation with DHA in SW620 cells suggest that relevant gene expression changes could occur very early.

We have previously performed gene expression analysis of SW620 cells after treatment with DHA (70 µM) or vehicle for 0.5, 1, 3, 6, 12, 24 and 48 h. No significant changes in gene expression were observed until 3 h after DHA supplementation [33]. At 3 h, 21 transcripts

were found differentially expressed; 17 of these were up-regulated, whereas 5 were down-regulated (data not shown). Among the earliest DHA-responsive transcripts was SQSTM1 (Table 1). The autophagy cargo receptor SQSTM1 physically links misfolded, ubiquitinated proteins to ATG8-family members located on the forming autophagosomal membrane [29, 30]. At 3 h, we also identified increased mRNA levels of the Bcl2-associated athanogene 3 (BAG3), as well as the chaperones Heat shock protein 40 (Hsp40) and Hsp70, the oxidative stress response gene HMOX1 and the ER stress response gene REDD1. After 6 h with DHA, 16 of the 21 transcripts were still differentially expressed. Moreover, an increased number of transcripts were differentially expressed at 6 h; 859 were up-regulated and 587 were down-regulated. The immediate activation of SQSTM1 and BAG3 may suggest induction of autophagy as a primary transcriptional response to DHA. In line with this, several ATG transcripts, including microtubule-associated protein 1 light chain 3 beta (LC3B) and its homologues GABA(A) receptor-associated protein like 1 (GABARAP-L1 and -L2), ATG14, as well as the autophagy regulators ULK1, sestrin 2 (SESN2) and Tribbles homolog 3 (TRIB3) were found to be significantly up-regulated ($p<0.05$) after 6 h DHA-treatment. Previous obtained gene expression data of SW620 cells treated with DHA for longer periods of time (12, 24 and 48 h) [14] also revealed increased mRNA levels of ATG12, BCL2/adenovirus E1B 19kDa interacting protein 3-like (Bnip3L/Nix), and phosphoinositide-3-kinase class 3 (Vps34). For complete lists of differentially expressed genes, see ArrayExpress accession numbers E-MEXP-2010 and E-MEXP-1014.

Results from gene expression analyses were verified by measuring protein levels of selected targets (SQSTM1, HSPA1A, HMOX1, TRIB3 and BAG3) in SW620 and Caco-2 cells after DHA-treatment for 3-48 h (Fig. 2). These analyses demonstrated a correlation between increased mRNA and protein level for these gene products. The protein level of SQSTM1, HSPA1A, HMOX1 and BAG3 increased with time up to 24 h in SW620 cells, while the same

transcripts were much less affected in Caco-2 cells, except for HMOX1. HMOX1 was found expressed in Caco-2 control cells, and increased with time up to 12 h, followed by a decrease at 24 and 48 h. HMOX1 was not expressed in SW620 control cells, but was found expressed after 6 h treatment with DHA. The expression increased up to 24 h and to a higher extent when compared to Caco-2 cells, before decreasing at 48h.

DHA induces a rapid increase in cellular ROS and nuclear import of NFE2L2 in the SW620 colon cancer cells

HMOX1 and SQSTM1 have previously been found to be induced by ROS via activation of the transcription factor NFE2L2 [34]. In the DHA-sensitive SW620 cells, an increase in ROS was observed already after 3 h of DHA-supplementation and a further increase was observed up to 24 h (Fig. 3A). Similarly, a clear increase in mitochondrial superoxide was detected in response to DHA in SW620 cells (Fig. 3B). However, the antioxidant vitamin E was not able to counteract DHA-induced formation of ROS in SW620 cells (Fig. 3C) and had no effect on cell survival (data not shown). Also, the two antioxidants BHA and BHT were not able to counteract the growth-inhibitory effect of DHA in SW620 cells (data not shown). In line with this, vitamin E supplementation did not interfere with DHA-induced nuclear translocation of NFE2L2 in these cells (data not shown). In contrast, the ROS-level in Caco-2 cells was elevated only after prolonged treatment (24 h) of DHA when using the superoxide probe and to a much lesser extent (not significant). We therefore measured the level of malondialdehyde (MDA), a secondary product of lipid peroxidation, in Caco-2 cells after treatment with DHA alone or in combination with vitamin E (50 µM) for 72 h (Fig. 3D). A several fold increase in the MDA level was observed in Caco-2 cells after DHA treatment (70 µM) for 72 h compared to control cells. Co-treatment with DHA (70 µM) and vitamin E (50 µM) reduced the level of MDA, but not to the same level as in control cells (Fig. 3D). We have previously measured

the level of MDA in SW620 cells under the same conditions [12]. The level of MDA was increased several fold in SW620 cells after treatment with DHA (70 μM) and a combinatory treatment with vitamin E (50 μM) reduced the level of MDA even below that in control cultures. These results indicate that oxidative stress and lipid peroxidation are induced by DHA-supplementation in both cell lines, although to different extents and at different time-points.

NFE2L2 is a major regulator of transcription of antioxidant related genes. We determined the total protein level of NFE2L2 by immunostaining and found a significant higher level of NFE2L2 in SW620 cells as compared to Caco-2 cells (Fig 4B). A clear nuclear translocation of NFE2L2 could be observed in the SW620 cells after 6 h of DHA treatment by confocal imaging (Fig. 4A), at the same time as we observed accumulation of SQSTM1 protein (Fig. 2A). Even though ROS could not be detected at early time points in Caco-2 cells, an increased nuclear translocation of NFE2L2 in the Caco-2 cells could be observed after 6 h treatment (Fig. 4A). These results indicate that the antioxidant defense system is activated in both cell lines after DHA-supplementation. Also, the level of KEAP1, a negative regulator of NFE2L2, was found lower in Caco-2 cells compared to SW620 cells (Fig. 4C). Together, these results demonstrate that NFE2L2 is translocated to the nucleus in both SW620 and Caco-2 cells, but that the level of ROS induction and growth retardation in response to DHA is clearly different between the two cell lines.

Basal autophagy is low and not induced by DHA in SW620 colon cancer cells

To determine whether DHA could affect autophagy, the autophagy biomarkers LC3B and SQSTM1 were immunostained. The number of LC3B punctuated structures per cell as well as LC3B-SQSTM1 double positive structures was found to be clearly higher in Caco-2 control cells compared to SW620 control cells (Fig. 5A). By adding bafilomycin A1 (BafA1) to

inhibit lysosomal degradation, a clear increase in both the number of punctuated structures positive for LC3B per cell and the number of SQSTM1-LC3B double-positive structures could be observed in both cell lines, although to a much larger extent in Caco-2 cells. These results suggest a higher basal autophagy in Caco-2 cells as compared to SW620 cells. DHA treatment did not significantly change the number LC3B punctuated structures in any of the two cell lines, suggesting that there is no induction of autophagy in response to DHA supplementation in these colon cancer cell lines. On the other hand, amino acid starvation of SW620 cells for 3 h caused an increase in the number of pixels positive for LC3B and of cytosolic structures positive for both LC3B and SQSTM1 (Fig. 5B). Combining amino acid starvation and inhibition of lysosomal degradation resulted in a synergistic raise in the number of autophagic structures positive for both proteins, indicating that autophagy may be induced in these cells, given the appropriate stimuli.

Autophagic flux was further analyzed by LC3B and SQSTM1 immunoblots of SW620 and Caco-2 cell extracts after treatment with DHA from 2 to 16 h in the absence or presence of BafA1 (Fig. 5C). Analyzing LC3B-II protein level indicated no increase in autophagic flux by DHA-supplementation in either cell line (Fig. 5C). However, the protein level of SQSTM1 was induced in both cell lines even though the autophagic flux remained unaffected for the time frame of the experiment (Fig. 2 and Fig. 5C). Also, the immunoblot analysis revealed that the basal level of LC3B-II (relative to actin) was approximately 10 fold higher in the Caco-2 cells compared to the SW620 cells (Fig. 5D). The basal level of SQSTM1 was found equal. The higher basal level of LC3B-II was not due to a blockade of autophagy in the Caco-2 cells, because the level was increased even further after inhibiting lysosomal activity (Fig 5E). Autophagy was also quantified as incorporation of the fluorescent autophagy related probe Cyto-ID detected by flow cytometry. These analyses revealed that Caco-2 cells displayed a more than 8-fold higher intensity per cell compared to the SW620 cells (Fig. 5F).

Consistent with the immunoblot analyses, DHA did not cause any significant increase in CytoID incorporation in SW620 or Caco-2 (data not shown).

We have previously generated a double tag construct composed of mCherry fused to EGFP [30]. This fusion protein is pH sensitive, since mCherry is very pH-stable whereas EGFP is labile and loses its fluorescence in the acidic lysosomes. The double tag protein showed very different pattern distribution between SW620 and Caco-2 cells, with strong accumulation in the nucleus of Caco-2 cells. Fused to SQSTM1 it locates in cytoplasmic punctuated structures representing both protein aggregates (green and red), neutral autophagosomes (green and red) and acidified lysosomes (red only). Transient expression of the mCherry-EGFP-SQSTM1 protein clearly demonstrated a higher number of red-only structures in the Caco-2 cells compared to the SW620 cells (Fig. 6). In addition, the frequency of cells with more acidic structures than green structures was clearly higher in the Caco-2 cells. In response to DHA there was an increase in the number of punctuated structures that were both green and red in both cell lines. Based on size, shape and fluorescent color, many of these DHA-induced structures with tagged SQSTM1 were most likely protein aggregates. Altogether, these data show that DHA is not able to induce autophagy in these two cell lines. However, in response to DHA, there is an induction of endogenous SQSTM1 and formation of protein aggregates positive for SQSTM1. Importantly, the basal level of autophagy is higher in the Caco-2 cells compared to the SW620 cells. Collectively, these results demonstrate an inverse correlation between DHA sensitivity and basal autophagy in these colon cancer cell lines.

NFE2L2-induced stress response is not the cause of DHA-sensitivity in cancer cells

To investigate whether NFE2L2-induced stress responses is important for the effect of DHA in cancer cells, siRNA targeting NFE2L2 was used to knock down the protein in SW620 and Caco-2 cells. In both cell lines, DHA (70 and 140 μM) induces protein expression of NFE2L2

and SQSTM1 (Fig. 7A). Targeting NFE2L2 by siRNA transfection reduced the induction of NFE2L2 by DHA (70 and 140 µM) in both cell lines (Fig. 7B). A reduction of SQSTM1 was observed in both cell lines and the level of the autophagy biomarker LC3B-II in Caco-2 and SW620 control cells was increased after NFE2L2 down regulation, suggesting a compensatory role of increased autophagy (Fig. 7C). The increased level of LC3B-II was not due to autophagy inhibition, since there was a clear further increase in response to lysosomal inhibition by BafA1. Down regulation of NFE2L2 did not cause an increased sensitivity for DHA in SW620 and Caco-2 cells (Fig. 7G). Also, siRNA-mediated down regulation of SQSTM1 in Caco-2 cells did not cause increased sensitivity towards DHA even if the down regulation was very efficient (data not shown). As previously mentioned, HMOX1 is expressed in Caco-2 control cells in contrast to SW620 control cells (Fig. 7D). However, siRNA-mediated down-regulation of HMOX1 did not affect cell growth in either cell lines (Fig. 7G).

The level of autophagy is important for DHA-induced toxicity

To determine whether basal autophagic flux was important for the sensitivity towards DHA, ATG5 or a combination of ATG5 and ATG7 was targeted by siRNA in Caco-2 cells (Fig. 7E/F). By combining siRNA targeting both ATG5 and ATG7, a tenfold reduction of the LC3B-II protein level was observed (Fig. 7E). Caco-2 cells transfected with ATG5 and ATG7 siRNA demonstrated reduced cell index compared to the non-targeting transfected cells in the presence of DHA (Fig. 7F). DHA sensitivity in ATG5 and ATG7 knock down cells were analyzed by conventional cell counting in both SW620 and Caco-2 cells and was found to be increased in both cell lines to almost the same extent (Fig. 7G). Importantly, in the absence of DHA, the ATG5 or ATG7 siRNA transfected cells did not grow slower than the control siRNA transfected cells. Consistent with the hypothesis that basal autophagy is important for

survival during DHA exposure, increasing the autophagic flux in SW620 and Caco-2 cells, using rapamycin, reduced the DHA sensitivity (Fig. 8A/B). In line with these findings, we show that by inhibiting autophagy with chloroquine, an increased sensitivity towards DHA is observed in Caco-2 cells (Fig. 8C). The protein expression level of the autophagy markers LC3B-II and/or SQSTM1 respond accordingly (Fig. 8B/C).

Collectively, these results suggest that basal autophagy is important for the DHA-sensitivity in these cancer cells.

Discussion

DHA was found to induce several autophagy-related transcripts at early time points in SW620 colon cancer cells that are growth inhibited by DHA; among these are SQSTM1 and BAG3 followed by LC3B, GABARAPL1 and ULK1. However, in SW620 cells the induced transcription of autophagy related genes did not result in a corresponding activation of autophagy, and we find a low level of autophagy both prior to and after DHA supplementation in these cells. Caco-2 cells, with higher DHA-tolerance, display a much higher basal autophagy, both in the presence and absence of DHA. The lack of increased autophagic flux in response to DHA in SW620 cells was surprising, because we have previously demonstrated a clear activation of both ER stress [14] and ROS-accumulation [12]; processes that are well documented to cause activation of autophagy. Indicative of ER-stress, several downstream targets of PERK like ATF4 and DNA damage-inducible protein 3 (DDIT3/CHOP), were found to be induced in SW620 cells; both ATF4 and CHOP may induce the expression of autophagy genes [14, 35].

The increased expression of autophagy genes in the SW620 cells in response to DHA could be a sign of a transcriptionally encoded response to counteract accumulation of damaged proteins. The finding that these cancer cells do not increase the autophagic flux indicates that

this transcriptional response is blocked at a translational or post-translational stage. We have previously found increased phosphorylation of eIF2α, indicative of ER-stress and shut down of general translation, as early as 3 h after DHA supplementation [14]. ER stress and release of calcium are also known to induce autophagy [17]. The eIF2α/ATF4 pathway has previously been shown to mediate gene transcriptional activation of several autophagy genes in response to both amino acid starvation and ER-stress [36]. Further research is necessary to clarify the mechanisms by which eIF2*α* phosphorylation regulates autophagy in response to ER stress signals.

ROS may regulate autophagy both by transcriptional regulatory mechanisms and post translational modifications. Increased levels of ROS-induced stress response activates hypoxia inducible factor 1 (HIF-1), p53, forkhead box O3 (FOXO3) and NFE2L2 which then induce transcription of LC3B, BNIP3 and SQSTM1 [37]. Also, downstream targets of the ER stress sensor PERK induce expression of autophagy genes (*LCB* and *ATG5*) thereby increasing autophagic flux [37]. We find that SQSTM1 (3 h), NFE2L2 (6 h) BNIP3 (12 h) and FOXO3A (12 h) are induced after DHA supplementation in the SW620 cells, indicating that the transcriptional machinery of autophagy is active in these cells.

ROS have also been suggested to induce autophagy by directly controlling the enzymatic activity of ATG4 needed for maturation of LC3-family members and formation of LC3B-II-positive autophagosomes [18]. In addition, it was recently reported that ROS cause an AMP-dependent activation of AMPK [38]. This kinase is crucial for the control of autophagy. ULK1 is phosphorylated and activated by AMPK [39], and AMPK also inhibits mTOR to increase autophagic flux [15]. DHA-induced transcription of several autophagy-related genes may possibly act in concert with ROS-induced activation of AMPK, thereby causing a posttranslational activation of autophagy by increased ULK1 activity. In line with this notion, Jing *et al.* recently demonstrated that DHA causes an AMPK-dependent activation of

autophagy in human cervical cancer SiHa cells [40]. This increased autophagy is suggested to contribute to increased cytotoxicity in a wild type p53 dependent manner. We find however the difference in DHA-sensitivity to be independent of wild type p53, since both Caco-2 and SW620 cells lack wild-type p53 [41]. Amino acid starvation of SW620 cells shows that autophagy is inducible in these cells. However, we still do not know why there are no detectable activation of autophagy in the SW620 cells after DHA-induced ROS and activation of autophagy-related genes. Niso-Santano *et al.* recently published the unexpected finding that unsaturated fatty acids promote autophagy in a beclin 1- (BECN1) and phosphatidylinositol 3-kinase, class 3-independent (PIK3C3) manner that is accompanied by the redistribution of LC3B to Golgi-associated vesicles, thereby relying on an intact Golgi apparatus [42]. This remains to be elucidated in our systems.

A study by Shin et al. show that supplementation of prostate cancer cell lines harboring mutant p53 with DHA results in generation of mitochondrial ROS and increased autophagic flux, suggesting that DHA induces both autophagy and apoptosis in these cells [43]. In contrast to these results, we find that both SW620 and Caco-2 cells harboring mutant p53 predicted to be damaging or non-functional [41], do not increase autophagic flux in response to DHA. Why certain cancer cells are unable to accelerate autophagy in response to stressful situations and how common this feature is, is not known. However, mutations in the autophagy gene *Beclin1* are commonly found in cancers [44, 45]. Furthermore, negative regulators of autophagy, such as PI3K and AKT are established oncogenes, and vice versa, positive regulators of the process, such as PTEN and TSC1/TSC2 are tumor suppressors [16]. Mutations in these genes may contribute to an inability to accelerate autophagy upon exposure to stress. Whether this is the case for SW620 or Caco-2 cells remains to be elucidated. Regardless, as autophagy is not induced by DHA in either cell line, we find that the basal autophagy is a determinant as to whether the cells survive DHA exposure.

The three most commonly mutated oncogenes in colorectal cancer cells are *KRAS*, *BRAF* and *PI3KCA* [46]. Caco-2 cells harbor no mutations in these oncogenes, while SW620 cells harbor *KRAS* mutation. The signaling pathways RAS/PKA and RAS/ERK have been shown to be involved in the regulation of autophagy [47] and many cancer cell lines harboring RAS mutations have also been shown to have high levels of autophagy [48]. There is a strong relationship between KRAS mutation and the NF-κB signaling pathway. SW620 cells have a constitutive activation of NF-κB in contrast to Caco-2 cells, and when treating both cell lines with a NF-κB inhibitor, the proliferation of SW620 cells was significantly decreased while the proliferation of Caco-2 cells was unaffected [49]. We have previously shown that DHA-treatment (70 μM) reduces total protein level of NF-κB in SW620 cells [35]. The role of KRAS mutation and NF-κB signaling in the regulation of autophagy remains to be elucidated in our system.

SW620 cells demonstrate a robust production of ROS in response to DHA at early time points, whereas a significant increase in ROS measured as MDA was detected in Caco-2 cells after supplementation with DHA for 72 h. Vitamin E did not counteract DHA-induced ROS as measured in our systems and did not interfere with nuclear translocation of NFE2L2 in SW620 cells. Also, vitamin E was not able to restore cell growth, indicating that lipid peroxidation may not be the major cause of DHA-induced cytotoxicity in SW620 cells. In contrast, vitamin E was able to reduce the level of MDA in Caco-2 cells, but not below that in control cultures. Cancer cells may display differences in the antioxidant defense systems or differences in the metabolic pathways for PUFAs that may explain these observations. HMOX-1, well known to be induced by a variety of stress stimuli, may contribute to the cells antioxidant defense against stress induced by ROS and thereby their sensitivity towards DHA. Therefore, it is interesting that HMOX1 was expressed in Caco-2 control cells and not in the

DHA-sensitive SW620 control cells. However, knock-down of HMOX1 did not affect DHA-sensitivity of either cell lines, indicating that this is a more general stress indicator.

DHA has previously been found to induce ROS-dependent aggregation and autophagic destruction of misfolded apolipoprotein B in hepatocytes [50]. Our findings suggest that DHA induces oxidative stress that may result in protein damage. The results from the double tag experiments demonstrated increased levels of protein aggregates positive for SQSTM1 in response to DHA. The rapid production of ROS and activation of NFE2L2 suggest increased ROS as an early response to PUFAs in SW620 cells. Subsequently, this ROS increase could contribute to protein misfolding and ER stress [51]. A close connection between these stress conditions is also illustrated by the important role of NFE2L2 in cell survival after ER stress [52]. However, it is difficult to separate these two intertwined stress conditions, and we have currently no firm data that demonstrate which controls the other upon DHA exposure.

Addition of DHA was found to cause a rapid stabilization and nuclear translocation of NFE2L2 in both SW620 and Caco-2 cells. In spite of this, we observed only a small increase (not significant) in ROS for the superoxide probe after prolonged exposure in the Caco-2 cells. NFE2L2 activation is negatively regulated by KEAP1. The cellular level of KEAP1 was recently shown to be controlled by autophagy; SQSTM1 makes a direct interaction and targets KEAP1 for lysosomal destruction [31, 32]. Thus, in cells with a high level of SQSTM1 and autophagy, KEAP1 is rapidly degraded leading to activation of NFE2L2. In line with this, we found the basal level of KEAP1 to be lower in Caco-2 cells compared to SW620 cells. Importantly, the affinity of SQSTM1 for KEAP1 was recently shown to be regulated by phosphorylation of SQSTM1 [53]. This phosphorylation of SQSTM1 and the resulting activation of NFE2L2 were found to be induced by diverse cellular stress conditions including arsenate and mitochondrial inhibition and to be rapamycin sensitive. As mentioned earlier, NFE2L2 is also regulated by phosphorylation by PERK after ER stress [28]. The stabilization

and nuclear translocation of NFE2L2 could therefore be mediated by such an alternative mechanism in response to DHA.

Several age-related diseases are associated with elevated levels of damaged mitochondria and protein aggregates [54, 55]. Stimulation of autophagy leads to reduced accumulation of such dysfunctional cellular components [56]. Autophagy acts pro-survival by clearing cells for damaged components and may thereby mobilize a disease preventive effect. This is in line with our findings showing that stimulation or inhibition of autophagy by rapamycin or chloroquine respectively, affects the DHA-induced toxicity in our system. Our data suggest that in cancer cells where the autophagy response may be defective or down regulated, DHA may cause growth retardation and/or cell death.

The frequency of tumors composed of cancer cells with down-regulated or loss of autophagy is currently not known. Unfortunately, there are currently limited possibilities to determine the actual autophagic flux in clinical samples of solid tumors, and the understanding of the role of autophagy in cancer development is still incomplete.

To test if the autophagic flux is affected after DHA supplementation *in vivo*, biomarkers that allow quantification of autophagy in clinical samples are needed. With such, we can evaluate if and how the process might change in response to intake of n-3 PUFAs in both normal and cancer cells. Development of diagnostic tools of autophagy and autophagy regulators is also needed in order to test the hypothesis that cancer cells with loss of autophagy could be sensitive for DHA in clinical settings.

Acknowledgements

We thank Terje Johansen and Hans Krokan for discussions and comments. Gene expression profiling was performed at the Norwegian Microarray consortium (NMC) in Trondheim. We thank Cathrine Goberg Olsen for gene expression profiling, Turid Follestad for the statistical

analysis, Lena Pape, Nina Beate Liabakk, Kamilla Zub and Ida Johansson for their experimental input. This work was supported by grants from The Faculty of Medicine, NTNU, the Norwegian Cancer Society, the Cancer Research Foundation at St. Olav Hospital, the Central Norway Regional Health Authority and The Research Council of Norway through "Småforsk" grant.

References

[1] Dyerberg, J. Coronary heart disease in Greenland Inuit: a paradox. Implications for western diet patterns. *Arctic Med Res* **48:**47-54; 1989.
[2] Friedland, R. P. Fish consumption and the risk of Alzheimer disease: is it time to make dietary recommendations? *Arch Neurol* **60:**923-924; 2003.
[3] Caygill, C. P.; Hill, M. J. Fish, n-3 fatty acids and human colorectal and breast cancer mortality. *Eur J Cancer Prev* **4:**329-332; 1995.
[4] Serini, S.; Fasano, E.; Piccioni, E.; Cittadini, A. R.; Calviello, G. Differential anti-cancer effects of purified EPA and DHA and possible mechanisms involved. *Curr Med Chem* **18:**4065-4075; 2011.
[5] Norat, T.; Bingham, S.; Ferrari, P.; Slimani, N.; Jenab, M.; Mazuir, M.; Overvad, K.; Olsen, A.; Tjonneland, A.; Clavel, F.; Boutron-Ruault, M. C.; Kesse, E.; Boeing, H.; Bergmann, M. M.; Nieters, A.; Linseisen, J.; Trichopoulou, A.; Trichopoulos, D.; Tountas, Y.; Berrino, F.; Palli, D.; Panico, S.; Tumino, R.; Vineis, P.; Bueno-de-Mesquita, H. B.; Peeters, P. H.; Engeset, D.; Lund, E.; Skeie, G.; Ardanaz, E.; Gonzalez, C.; Navarro, C.; Quiros, J. R.; Sanchez, M. J.; Berglund, G.; Mattisson, I.; Hallmans, G.; Palmqvist, R.; Day, N. E.; Khaw, K. T.; Key, T. J.; San Joaquin, M.; Hemon, B.; Saracci, R.; Kaaks, R.; Riboli, E. Meat, fish, and colorectal cancer risk: the European Prospective Investigation into cancer and nutrition. *J Natl Cancer Inst* **97:**906-916; 2005.
[6] Kato, I.; Akhmedkhanov, A.; Koenig, K.; Toniolo, P. G.; Shore, R. E.; Riboli, E. Prospective study of diet and female colorectal cancer: the New York University Women's Health Study. *Nutrition and cancer* **28:**276-281; 1997.
[7] Bathen, T. F.; Holmgren, K.; Lundemo, A. G.; Hjelstuen, M. H.; Krokan, H. E.; Gribbestad, I. S.; Schonberg, S. A. Omega-3 fatty acids suppress growth of SW620 human colon cancer xenografts in nude mice. *Anticancer Res* **28:**3717-3723; 2008.
[8] Jensen, L. R.; Berge, K.; Bathen, T. F.; Wergedahl, H.; Schonberg, S. A.; Bofin, A.; Berge, R. K.; Gribbestad, I. S. Effect of dietary tetradecylthioacetic acid on colon cancer growth studied by dynamic contrast enhanced MRI. *Cancer Biol Ther* **6:**1810-1816; 2007.
[9] Cockbain, A. J.; Toogood, G. J.; Hull, M. A. Omega-3 polyunsaturated fatty acids for the treatment and prevention of colorectal cancer. *Gut* **61:**135-149; 2012.
[10] Hossain, Z.; Hosokawa, M.; Takahashi, K. Growth inhibition and induction of apoptosis of colon cancer cell lines by applying marine phospholipid. *Nutrition and cancer* **61:**123-130; 2009.
[11] Takahashi, M.; Fukutake, M.; Isoi, T.; Fukuda, K.; Sato, H.; Yazawa, K.; Sugimura, T.; Wakabayashi, K. Suppression of azoxymethane-induced rat colon carcinoma development by a fish oil component, docosahexaenoic acid (DHA). *Carcinogenesis* **18:**1337-1342; 1997.
[12] Schonberg, S. A.; Lundemo, A. G.; Fladvad, T.; Holmgren, K.; Bremseth, H.; Nilsen, A.; Gederaas, O.; Tvedt, K. E.; Egeberg, K. W.; Krokan, H. E. Closely related colon cancer cell lines display different sensitivity to polyunsaturated fatty acids, accumulate different lipid classes and downregulate sterol regulatory element-binding protein 1. *FEBS J* **273:**2749-2765; 2006.
[13] Slagsvold, J. E.; Pettersen, C. H.; Follestad, T.; Krokan, H. E.; Schonberg, S. A. The antiproliferative effect of EPA in HL60 cells is mediated by alterations in calcium homeostasis. *Lipids* **44:**103-113; 2009.
[14] Jakobsen, C. H.; Storvold, G. L.; Bremseth, H.; Follestad, T.; Sand, K.; Mack, M.; Olsen, K. S.; Lundemo, A. G.; Iversen, J. G.; Krokan, H. E.; Schonberg, S. A. DHA induces ER stress and growth arrest in human colon cancer cells: associations with cholesterol and calcium homeostasis. *J Lipid Res* **49:**2089-2100; 2008.
[15] Kroemer, G.; Marino, G.; Levine, B. Autophagy and the integrated stress response. *Mol Cell* **40:**280-293; 2010.

[16] Mizushima, N.; Levine, B.; Cuervo, A. M.; Klionsky, D. J. Autophagy fights disease through cellular self-digestion. *Nature* **451:**1069-1075; 2008.
[17] Hoyer-Hansen, M.; Bastholm, L.; Szyniarowski, P.; Campanella, M.; Szabadkai, G.; Farkas, T.; Bianchi, K.; Fehrenbacher, N.; Elling, F.; Rizzuto, R.; Mathiasen, I. S.; Jaattela, M. Control of macroautophagy by calcium, calmodulin-dependent kinase kinase-beta, and Bcl-2. *Mol Cell* **25:**193-205; 2007.
[18] Scherz-Shouval, R.; Shvets, E.; Fass, E.; Shorer, H.; Gil, L.; Elazar, Z. Reactive oxygen species are essential for autophagy and specifically regulate the activity of Atg4. *The EMBO journal* **26:**1749-1760; 2007.
[19] Liu, E. Y.; Ryan, K. M. Autophagy and cancer--issues we need to digest. *Journal of cell science* **125:**2349-2358; 2012.
[20] Mizushima, N. Autophagy: process and function. *Genes & development* **21:**2861-2873; 2007.
[21] Galluzzi, L.; Pietrocola, F.; Levine, B.; Kroemer, G. Metabolic control of autophagy. *Cell* **159:**1263-1276; 2014.
[22] Efeyan, A.; Zoncu, R.; Chang, S.; Gumper, I.; Snitkin, H.; Wolfson, R. L.; Kirak, O.; Sabatini, D. D.; Sabatini, D. M. Regulation of mTORC1 by the Rag GTPases is necessary for neonatal autophagy and survival. *Nature* **493:**679-683; 2013.
[23] Hosokawa, N.; Hara, T.; Kaizuka, T.; Kishi, C.; Takamura, A.; Miura, Y.; Iemura, S.; Natsume, T.; Takehana, K.; Yamada, N.; Guan, J. L.; Oshiro, N.; Mizushima, N. Nutrient-dependent mTORC1 association with the ULK1-Atg13-FIP200 complex required for autophagy. *Molecular biology of the cell* **20:**1981-1991; 2009.
[24] Dennis, M. D.; McGhee, N. K.; Jefferson, L. S.; Kimball, S. R. Regulated in DNA damage and development 1 (REDD1) promotes cell survival during serum deprivation by sustaining repression of signaling through the mechanistic target of rapamycin in complex 1 (mTORC1). *Cellular signalling* **25:**2709-2716; 2013.
[25] Motohashi, H.; Yamamoto, M. Nrf2-Keap1 defines a physiologically important stress response mechanism. *Trends in molecular medicine* **10:**549-557; 2004.
[26] Sekhar, K. R.; Yan, X. X.; Freeman, M. L. Nrf2 degradation by the ubiquitin proteasome pathway is inhibited by KIAA0132, the human homolog to INrf2. *Oncogene* **21:**6829-6834; 2002.
[27] Itoh, K.; Tong, K. I.; Yamamoto, M. Molecular mechanism activating Nrf2-Keap1 pathway in regulation of adaptive response to electrophiles. *Free radical biology & medicine* **36:**1208-1213; 2004.
[28] Cullinan, S. B.; Zhang, D.; Hannink, M.; Arvisais, E.; Kaufman, R. J.; Diehl, J. A. Nrf2 is a direct PERK substrate and effector of PERK-dependent cell survival. *Mol Cell Biol* **23:**7198-7209; 2003.
[29] Bjorkoy, G.; Lamark, T.; Brech, A.; Outzen, H.; Perander, M.; Overvatn, A.; Stenmark, H.; Johansen, T. p62/SQSTM1 forms protein aggregates degraded by autophagy and has a protective effect on huntingtin-induced cell death. *The Journal of cell biology* **171:**603-614; 2005.
[30] Pankiv, S.; Clausen, T. H.; Lamark, T.; Brech, A.; Bruun, J. A.; Outzen, H.; Overvatn, A.; Bjorkoy, G.; Johansen, T. p62/SQSTM1 binds directly to Atg8/LC3 to facilitate degradation of ubiquitinated protein aggregates by autophagy. *The Journal of biological chemistry* **282:**24131-24145; 2007.
[31] Jain, A.; Lamark, T.; Sjottem, E.; Larsen, K. B.; Awuh, J. A.; Overvatn, A.; McMahon, M.; Hayes, J. D.; Johansen, T. p62/SQSTM1 is a target gene for transcription factor NRF2 and creates a positive feedback loop by inducing antioxidant response element-driven gene transcription. *The Journal of biological chemistry* **285:**22576-22591; 2010.
[32] Komatsu, M.; Kurokawa, H.; Waguri, S.; Taguchi, K.; Kobayashi, A.; Ichimura, Y.; Sou, Y. S.; Ueno, I.; Sakamoto, A.; Tong, K. I.; Kim, M.; Nishito, Y.; Iemura, S.; Natsume, T.; Ueno, T.; Kominami, E.; Motohashi, H.; Tanaka, K.; Yamamoto, M. The selective autophagy substrate p62 activates the stress responsive transcription factor Nrf2 through inactivation of Keap1. *Nat Cell Biol* **12:**213-223; 2010.
[33] Storvold, G. L.; Fleten, K. G.; Olsen, C. G.; Follestad, T.; Krokan, H. E.; Schonberg, S. A. Docosahexaenoic acid activates some SREBP-2 targets independent of cholesterol and ER stress in SW620 colon cancer cells. *Lipids* **44:**673-683; 2009.
[34] Ishii, T.; Itoh, K.; Takahashi, S.; Sato, H.; Yanagawa, T.; Katoh, Y.; Bannai, S.; Yamamoto, M. Transcription factor Nrf2 coordinately regulates a group of oxidative stress-inducible genes in macrophages. *The Journal of biological chemistry* **275:**16023-16029; 2000.
[35] Slagsvold, J. E.; Pettersen, C. H.; Storvold, G. L.; Follestad, T.; Krokan, H. E.; Schonberg, S. A. DHA alters expression of target proteins of cancer therapy in chemotherapy resistant SW620 colon cancer cells. *Nutrition and cancer* **62:**611-621; 2010.
[36] B'Chir, W.; Maurin, A. C.; Carraro, V.; Averous, J.; Jousse, C.; Muranishi, Y.; Parry, L.; Stepien, G.; Fafournoux, P.; Bruhat, A. The eIF2alpha/ATF4 pathway is essential for stress-induced autophagy gene expression. *Nucleic acids research* **41:**7683-7699; 2013.
[37] Scherz-Shouval, R.; Elazar, Z. Regulation of autophagy by ROS: physiology and pathology. *Trends in biochemical sciences* **36:**30-38; 2011.

[38] Hawley, S. A.; Ross, F. A.; Chevtzoff, C.; Green, K. A.; Evans, A.; Fogarty, S.; Towler, M. C.; Brown, L. J.; Ogunbayo, O. A.; Evans, A. M.; Hardie, D. G. Use of cells expressing gamma subunit variants to identify diverse mechanisms of AMPK activation. *Cell Metab* **11:**554-565; 2010.
[39] Egan, D. F.; Shackelford, D. B.; Mihaylova, M. M.; Gelino, S.; Kohnz, R. A.; Mair, W.; Vasquez, D. S.; Joshi, A.; Gwinn, D. M.; Taylor, R.; Asara, J. M.; Fitzpatrick, J.; Dillin, A.; Viollet, B.; Kundu, M.; Hansen, M.; Shaw, R. J. Phosphorylation of ULK1 (hATG1) by AMP-activated protein kinase connects energy sensing to mitophagy. *Science* **331:**456-461; 2011.
[40] Jing, K.; Song, K. S.; Shin, S.; Kim, N.; Jeong, S.; Oh, H. R.; Park, J. H.; Seo, K. S.; Heo, J. Y.; Han, J.; Park, J. I.; Han, C.; Wu, T.; Kweon, G. R.; Park, S. K.; Yoon, W. H.; Hwang, B. D.; Lim, K. Docosahexaenoic acid induces autophagy through p53/AMPK/mTOR signaling and promotes apoptosis in human cancer cells harboring wild-type p53. *Autophagy* **7:**1348-1358; 2011.
[41] Ahmed, D.; Eide, P. W.; Eilertsen, I. A.; Danielsen, S. A.; Eknaes, M.; Hektoen, M.; Lind, G. E.; Lothe, R. A. Epigenetic and genetic features of 24 colon cancer cell lines. *Oncogenesis* **2:**e71; 2013.
[42] Niso-Santano, M.; Malik, S. A.; Pietrocola, F.; Bravo-San Pedro, J. M.; Marino, G.; Cianfanelli, V.; Ben-Younes, A.; Troncoso, R.; Markaki, M.; Sica, V.; Izzo, V.; Chaba, K.; Bauvy, C.; Dupont, N.; Kepp, O.; Rockenfeller, P.; Wolinski, H.; Madeo, F.; Lavandero, S.; Codogno, P.; Harper, F.; Pierron, G.; Tavernarakis, N.; Cecconi, F.; Maiuri, M. C.; Galluzzi, L.; Kroemer, G. Unsaturated fatty acids induce non-canonical autophagy. *The EMBO journal*; 2015.
[43] Shin, S.; Jing, K.; Jeong, S.; Kim, N.; Song, K. S.; Heo, J. Y.; Park, J. H.; Seo, K. S.; Han, J.; Park, J. I.; Kweon, G. R.; Park, S. K.; Wu, T.; Hwang, B. D.; Lim, K. The omega-3 polyunsaturated fatty acid DHA induces simultaneous apoptosis and autophagy via mitochondrial ROS-mediated Akt-mTOR signaling in prostate cancer cells expressing mutant p53. *BioMed research international* **2013:**568671; 2013.
[44] Yue, Z.; Jin, S.; Yang, C.; Levine, A. J.; Heintz, N. Beclin 1, an autophagy gene essential for early embryonic development, is a haploinsufficient tumor suppressor. *Proceedings of the National Academy of Sciences of the United States of America* **100:**15077-15082; 2003.
[45] Qu, X.; Yu, J.; Bhagat, G.; Furuya, N.; Hibshoosh, H.; Troxel, A.; Rosen, J.; Eskelinen, E. L.; Mizushima, N.; Ohsumi, Y.; Cattoretti, G.; Levine, B. Promotion of tumorigenesis by heterozygous disruption of the beclin 1 autophagy gene. *The Journal of clinical investigation* **112:**1809-1820; 2003.
[46] Forbes, S. A.; Bindal, N.; Bamford, S.; Cole, C.; Kok, C. Y.; Beare, D.; Jia, M.; Shepherd, R.; Leung, K.; Menzies, A.; Teague, J. W.; Campbell, P. J.; Stratton, M. R.; Futreal, P. A. COSMIC: mining complete cancer genomes in the Catalogue of Somatic Mutations in Cancer. *Nucleic acids research* **39:**D945-950; 2011.
[47] Kubisch, J.; Turei, D.; Foldvari-Nagy, L.; Dunai, Z. A.; Zsakai, L.; Varga, M.; Vellai, T.; Csermely, P.; Korcsmaros, T. Complex regulation of autophagy in cancer - integrated approaches to discover the networks that hold a double-edged sword. *Seminars in cancer biology* **23:**252-261; 2013.
[48] Guo, J. Y.; Chen, H. Y.; Mathew, R.; Fan, J.; Strohecker, A. M.; Karsli-Uzunbas, G.; Kamphorst, J. J.; Chen, G.; Lemons, J. M.; Karantza, V.; Coller, H. A.; Dipaola, R. S.; Gelinas, C.; Rabinowitz, J. D.; White, E. Activated Ras requires autophagy to maintain oxidative metabolism and tumorigenesis. *Genes & development* **25:**460-470; 2011.
[49] Lin, G.; Tang, Z.; Ye, Y. B.; Chen, Q. NF-kappaB activity is downregulated by KRAS knockdown in SW620 cells via the RAS-ERK-IkappaBalpha pathway. *Oncology reports* **27:**1527-1534; 2012.
[50] Pan, M.; Maitin, V.; Parathath, S.; Andreo, U.; Lin, S. X.; St Germain, C.; Yao, Z.; Maxfield, F. R.; Williams, K. J.; Fisher, E. A. Presecretory oxidation, aggregation, and autophagic destruction of apoprotein-B: a pathway for late-stage quality control. *Proceedings of the National Academy of Sciences of the United States of America* **105:**5862-5867; 2008.
[51] Malhotra, J. D.; Miao, H.; Zhang, K.; Wolfson, A.; Pennathur, S.; Pipe, S. W.; Kaufman, R. J. Antioxidants reduce endoplasmic reticulum stress and improve protein secretion. *Proceedings of the National Academy of Sciences of the United States of America* **105:**18525-18530; 2008.
[52] Cullinan, S. B.; Diehl, J. A. PERK-dependent activation of Nrf2 contributes to redox homeostasis and cell survival following endoplasmic reticulum stress. *J Biol Chem* **279:**20108-20117; 2004.
[53] Ichimura, Y.; Waguri, S.; Sou, Y. S.; Kageyama, S.; Hasegawa, J.; Ishimura, R.; Saito, T.; Yang, Y.; Kouno, T.; Fukutomi, T.; Hoshii, T.; Hirao, A.; Takagi, K.; Mizushima, T.; Motohashi, H.; Lee, M. S.; Yoshimori, T.; Tanaka, K.; Yamamoto, M.; Komatsu, M. Phosphorylation of p62 activates the Keap1-Nrf2 pathway during selective autophagy. *Mol Cell* **51:**618-631; 2013.
[54] Green, D. R.; Galluzzi, L.; Kroemer, G. Mitochondria and the autophagy-inflammation-cell death axis in organismal aging. *Science* **333:**1109-1112; 2011.
[55] Buchberger, A.; Bukau, B.; Sommer, T. Protein quality control in the cytosol and the endoplasmic reticulum: brothers in arms. *Mol Cell* **40:**238-252; 2010.
[56] Madeo, F.; Tavernarakis, N.; Kroemer, G. Can autophagy promote longevity? *Nat Cell Biol* **12:**842-846; 2010.

FIGURE LEGENDS

Fig. 1. Effect of DHA and OA on cell growth/cell index of the human colon cancer cell lines SW620 and Caco-2. Cell viability was assayed using the MTT assay. The experiment was performed in triplicate and the values represent the mean ± SD. Cell index was measured real-time by the xCELLigence system. The cell index is based on triplicate measurements and the normalized cell index curves are one representative out of two parallel experiments.

Fig. 2. Western blot analyses of proteins involved in autophagy from total cell extracts of SW620 and Caco-2 cells treated with DHA (70 μM) for indicated time periods (h). Controls were harvested at all times points, only 24 h control is shown and set to 1. Results were verified in three independent experiments; one representative blot is shown. Protein band intensities, normalized against ACTB are displayed and represent mean fold change (SD) of DHA samples relative to control at the indicated time points for three independent experiments. *Significantly different from control at the same time point (student's t-test, $p<0.05$).

Fig. 3. DHA-induced oxidative stress in SW620 and Caco-2 cells. (A) Changes in ROS levels measured at different time points after DHA treatment (70 μM) by the fluorescent probe DCF. Data represent mean intensity (±SD) of 10,000 cells per condition and are averaged from more than three independent experiments for the 3 h and 6 h and two independent experiments for the 24 h time point. *Significantly different from control (student's t-test $p<0.05$). (B) Cellular superoxide production detected by the mitochondrial targeted MitoSOX probe following DHA-treatment (70 μM) or vehicle. The mean MitoSOX intensity in 10,000

cells after 6 h with vehicle was set to 1 for SW620 and Caco-2, and displayed as the mean (±SD) of three independent experiments for the 3 h and 6 h and two independent experiments for the 24 h time point. *Significantly different from control (student's t-test, $p<0.05$). (C) The level of cellular ROS in 10,000 SW620 cells in triplicate wells per condition was determined using the DCF and MitoSOX probe by flow cytometry. The cells were treated with only DHA (70 μM, 3 h), preincubated with vitamin E (50 μM, 16 h) before DHA-treatment (70 μM, 3 h) or pretreated with vitamin E (50 μM, 16 h) and then co-incubated with DHA (70 μM, 3 h). The values represent the mean (±SD) of triplicate measurments in one experiment. (D) Lipid peroxidation measured as MDA in Caco-2 cells treated with DHA (70 μM) alone or in combination with vitamin E (50 μM) for 72 h. The values represent the mean ± SD of three independent experiments. *Significantly different from control, **significantly different from control and DHA treated cells (student's t-test $p<0.05$).

Fig. 4. DHA-induced activation of NFE2L2 in SW620 and Caco-2 cells. (A) Immunostaining of NFE2L2 in SW620 and Caco-2 cells after DHA (70 μM) or vehicle treatment for 6 h. Nuclear DNA was stained using Draq 5. Scale bar, 10 μm. The percentage of cells with equal or increased staining of NFE2L2 in the nucleus (N) was scored by microscopy of more than 60 cells for each condition. The results are representative for more than three independent experiments. (B) Immunoblot analysis of total NFE2L2 in total extracts of SW620 and Caco-2 cells. COX IV was used as a loading control and one representative blot is shown. The blots were quantified and intensities normalized relative to loading control. The number under the blot represents mean fold change (SD) of three independent experiments relative to the level in Caco-2 cells which was set to one. *Significantly different from Caco-2 cells (student's t-test, $p<0.05$). (C) Immunoblot analysis of KEAP1 in total cell extracts of SW620 and Caco-2

cells. The basal level of KEAP1 relative to tubulin (TUBB) was determined in six independent experiments. *Significantly different from SW620 cells (student's t-test, $p<0.05$).

Fig. 5. The level of basal autophagy is low in SW620 compared to Caco-2 colon cancer cells. (A) Immunostaining of SQSTM1 and LC3B after 6 h of vehicle, DHA (70 μM), BafA1 (200 nM) or a combination of the two. (B) Co-localization between SQSTM1 and LC3B in SW620 cells after 6 h of amino acid starvation (HBSS) in the presence or absence of BafA1 (200 nM). The amount of LC3B in autophagy-related punctuated cytoplasmic structures were quantified as the number of positive pixels (with more than 100 RLU) per cell in more than 100 cells for each condition. The relative differences between treated and untreated cell cultures are representative for more than five independent experiments. Scale bar: 20 μm. (C) Immunoblotting of LC3B-II and SQSTM1 in response to DHA observed at different times of BafA1 (100 nM) treatment in SW620 cells (60 μg total protein per well) and Caco-2 cells (40 μg total protein per well). ACTB was used as a loading control. Values represent the mean (± SD) of three independent experiments. *Significantly different from 0 h, **Significantly different from 0 h and BAFA1 at same time point (student's t-test, $p<0.05$). (D) The basal level of SQSTM1 and LC3B-II normalized to the level of ACTB in Caco-2 cells relative to the level in SW620 cells determined by immunoblotting in four independent experiments. The relative level of p62 and LC3B-II in SW620, respectively, were set to one and the relative level in Caco-2 determined in extracts made from untreated cells. (E) Protein levels of LC3B-II in SW620 and Caco-2 cells determined by immunoblotting of total cell extracts (60 μg) after BafA1 (100 nM) treatment at the indicated time points. Results were normalized to ACTB and related to the 0 h time point in three independent experiments. (F) Differences in the incorporation of the autophagy related probe CytoID in untreated SW620 and Caco-2 cells

measured by flow cytometry. Results are mean intensity of 10,000 single cells from triplicate measurements of each cell type from three independent experiments (±SD).

Fig.6. The localization pattern of mCherry-EGFP (CG) tagged SQSTM1 in Caco-2 and SW620 cells. Cells expressing the CG double tag alone or fused with SQSTM1 for 24 h were left untreated or exposed to DHA (70 μM) for 16 h before fixation and confocal imaging. The cells are representative for more than 300 single cells evaluated for each condition. Scale bar 10 μm.

Fig. 7. The effect of knocking down the redox-sensitive transcription factor NFE2L2, HMOX1 and autophagy on DHA sensitivity in SW620 and Caco-2 cells. (A) Level of NFE2L2 and SQSTM1 after supplementation with DHA (70 and 140 μM). (B) Level of NFE2L2 after treatment with siRNA targeting NFE2L2 in SW620 and Caco-2 cells (50 and 20 nM, respectively). Cells were transfected with siRNA and left for 24 h before re-seeding. Following incubation for 24 h, the cells were added DHA (70 μM or 140 μM) for 16 h. Results are based on triplicate experiments (±SD) for SW620 cells and for Caco-2 cells results from one representative experiment is shown. *Significantly different from its respective control (student's t-test, $p<0.05$). (C) Down regulation of NFE2L2 causes changes in the protein level of SQSTM1 and LC3B-II after treatment with BafA1 (100 nM) for different time periods in SW620 and Caco-2 cells. Values represent the mean (±SD) of three independent experiments, except for two independent experiments for protein levels of SQSTM1 in Caco-2 cells. *Significantly different from non-targeting (NT) at 0 h, **significantly different from NT 0 h and its respective NT (student's t-test, $p<0.05$). (D) Level of HMOX1 after treatment with siRNA targeting HMOX1 (100 nM) in SW620 and Caco-2 cells. Cells were transfected with siRNA and left for 24 h before re-seeding.

Following incubation for 24 h, the cells were added DHA (70 μM) for 16 h. Results represent mean (±SD) of three independent experiments for SW620 and Caco-2 cells. *Significantly different from NT DHA (70 μM) for SW620 cells, significantly different from NT control for Caco-2 cells, **significantly different from NT control and its respective NT (student's t-test, $p<0.05$). (E) Levels of LC3B-II and SQSTM1 following ATG5 (100 nM total), ATG5 and ATG7 (50 nM of each) or NT (100 nM) siRNA in Caco-2 cells treated with BafA1 (100 nM) for 2 h. The level of the respective proteins in the NT cells was set to one and the level is indicated below each protein band. (F) Relative changes in cell index of DHA-treated (140 μM) Caco-2 cells transfected with NT, ATG5 or a combination of ATG5 and ATG7 siRNA based on real-time monitoring using the xCELLigence instrument. The cell index for the DHA-treated NT siRNA transfected cells were used for normalization. The relative differences in cell index based on three independent experiments performed in triplicates and quantified by xCELLigence. (G) Relative differences in cell numbers (cell counting) for DHA-treated (70 μM) SW620 and Caco-2 cells upon down regulation of HMOX1, NFE2L2 and Atg5/7 by siRNA. *Significantly different from NT DHA (70 μM) (student's t-test, $p<0.05$)

Fig. 8. Induction of autophagy reduces DHA sensitivity and inhibition of autophagy increases DHA sensitivity. (A) Normalized cell index estimates of SW620 cells treated with rapamycin (50 nM), DHA (70 μM) or a combination using the xCELLigence instrument. The cell index was normalized to the last measurement before treatment. Changes in basal autophagic flux in the SW620 cells were determined by immunoblot for LC3B-II and SQSTM1 after treatment with rapamycin (50 nM), BafA1 (100 nM) or a combination for 24 h (insert with quantifications below). (B) Relative changes in cell index estimates for Caco-2 cells treated with DHA (105 μM) alone or in combination with rapamycin (50 nM) for 24 and 48 h.

Significant results representative of three independent experiments (with SD) performed in triplicates and quantified by xCELLigence (student's t-test, $p<0.05$). Relative changes in Caco-2 cell numbers (cell counting) upon the same treatments for 48 h. Results presented as mean (±SD) of three independent experiments (student's t-test, $p<0.05$). Changes in autophagic flux in the Caco-2 cells were determined by immunoblot for LC3B-II after treatment with rapamycin (50 nM), BafA1 (100 nM) or a combination for 24 h. Results are representative for 3 independent experiments, *significantly different from BafA1 alone (student's t-test, $p<0.05$). C) Relative changes in cell index and cell number for Caco-2 cells treated with DHA (70 µM) alone or in combination with chloroquine (10 µM) for indicated time points using the xCELLigence instrument or cell counting respectively. The cell index was normalized to the last measurement before treatment. Results presented as mean (±SD) of three independent experiments (student's t-test, $p<0.05$). Changes in autophagic flux in the Caco-2 cells were determined by immunoblot for LC3B-II and SQSTM1 after treatment with chloroquine (10 µM), BafA1 (100 nM) or a combination for indicated time points.

TABLE 1. Differentially expressed transcripts involved in autophagy and oxidative stress response in SW620 cells after treatment with DHA (70 μM) at time points indicated

Gene symbol	Affymetrix ID	Refseq NCBI ID	Transcript name	Fold change				
				3 h	6 h	12 h	24 h	48 h
ATG1/ULK1	209333_at	NM_003565	Unc-51-like kinase 1 (C. elegans)	NC	2.1	2.3	2.3	NC
ATG1/ULK1	238042_at	AW_134485	Unc-51-like kinase 1 (C. elegans)	NC	1.9	NA	NA	NA
ATG12	213026_at	NM_004707 NR_033362 NR_033363	Autophagy related 12 homolog (S. cerevisiae)	NC	NC	1.4	NC	NC
ATG14	204568_at	NM_014924	Autophagy related 14 homolog (S. cerevisiae)	NC	1.3	NA	NA	NA
BAG3	217911_s_at	NM_004281	BCL2-associated athanogene 3*	1.9	3.5	9.9	5.4	NC
BNIP3L/NIX	221479_s_at	NM_004331	BCL2/adenovirus E1B 19kDa interacting protein 3-like	NC	NC	1.5	1.8	NC
DNAJB1	200666_s_at	NM_006145	DnaJ (Hsp40) homolog, subfamily B, member 1	2.2	4.1	8.0	4.1	NC
DDIT4/REDD1	202887_s_at	NM_019058	DNA-damage-inducible transcript 4	5.5	23.1	NA	NA	NA
FOXO3A	204131_s_at	NM_001455 NM_201559	Forkhead box O3	NC	NC	1.3	1.4	1.3
HMOX1	203665_at	NM_002133	Heme oxygenase (decycling) 1*	3.2	25.6	24.0	10.6	5.7
HSPA1A	200799_at	NM_005345	Heat shock 70kDa protein 1A	4.5	4.1	NA	NA	NA
HSPA1A/B	200800_s_at 202581_at	NM_005345 NM_005346	Heat shock 70kDa protein 1A/1B*	4.4 5.4	6.5 4.5	17.8 9.8	9.8 6.5	5.1 3.1
GABARAPL1	208868_s_at 208869_s_at	NM_031412	GABA(A) receptor-associated protein like 1	NC NC	1.4 2.0	NA NA	NA NA	NA NA
GABARAPL1/L3	211458_s_at	NM_031412 NR_028287	GABA(A) receptor-associated protein like 1 / 3	NC	3.1	NA	NA	NA
GABARAPL2/ATG8	209046_s_at	NM_007285	GABA(A) receptor-associated protein-like 2	NC	NC	NC	1.2	NC
MAP1LC3B	208786_s_at	NM_022818	Microtubule-associated protein 1 light chain 3 beta	NC	2.4	NC	NA	NA
MAP1LC3B2	208785_s_at	NM_022818	Microtubule-associated protein 1 light chain 3 beta	NC	1.9	NC	3.9	2.3
NBR1	201384_s_at	NM_005899 NM_031858 NM_031862	Neighbour of BRCA1 gene 1	NC	NC	NC	1.6	1.4
NFE2L2/NRF2	201146_at	NM_001145412 NM_001145413 NM_006164	Nuclear factor (erythroid-derived 2)-like 2*	NC	1.5	2.0	1.8	NC
PIK3C3/Vps34	204297_at	NM_002647	Phosphoinositide-3-kinase, class 3	NC	NC	1.6	1.7	NC

SESN2	223195_s_at	NM_031459	Sestrin 2	NC	6.9	NA	NA	NA
	223196_s_at			NC	4.2	NA	NA	NA
SQSTM1/p62	201471_s_at	NM_001142298	Sequestosome 1*	NC	2.4	6.7	7.3	3.9
	213112_s_at	NM_001142299		NC	3.0	7.7	6.7	5.0
	244804_at	NM_003900		2.4	3.4	NA	NA	NA
TRIB3	218145_at	NM_021158	Tribbles homolog 3 (Drosophila)*	NC	4.0	7.4	6.5	3.3
	1555788_a_at			NC	5.25	NA	NA	NA

NC: No change. NA: Not on array. *: Already published

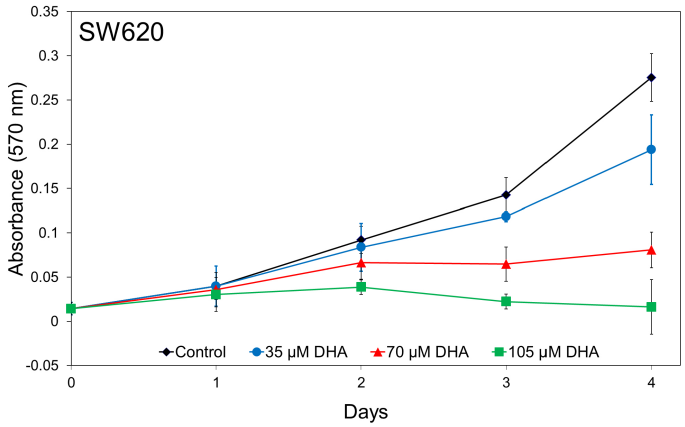
SW620
Absorbance (570 nm)
0.35
0.3
0.25
0.2
0.15
0.1
0.05
0
-0.05
0
1
2
3
4
Days
Control
35 μM DHA
70 μM DHA
105 μM DHA

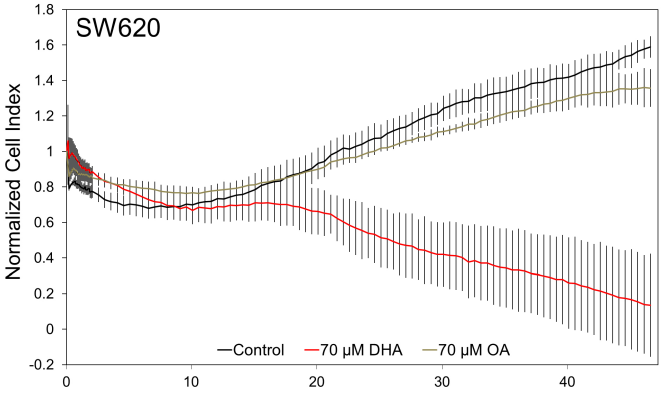
SW620
Normalized Cell Index
1.8
1.6
1.4
1.2
1
0.8
0.6
0.4
0.2
0
-0.2
0
10
20
30
40
Control
70 μM DHA
70 μM OA

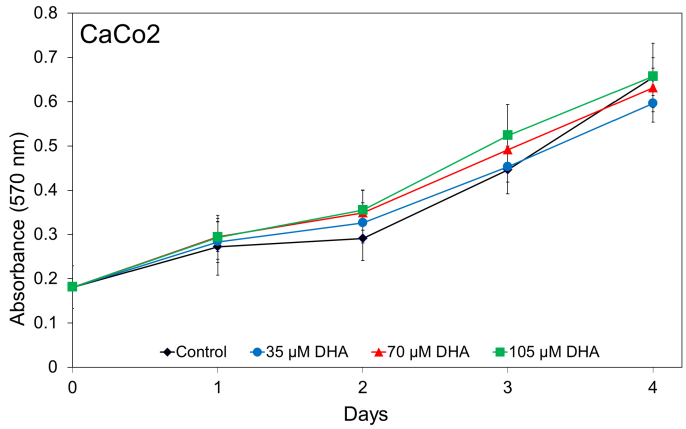
CaCo2
Absorbance (570 nm)
0.8
0.7
0.6
0.5
0.4
0.3
0.2
0.1
0
0
1
2
3
4
Days
Control
35 μM DHA
70 μM DHA
105 μM DHA

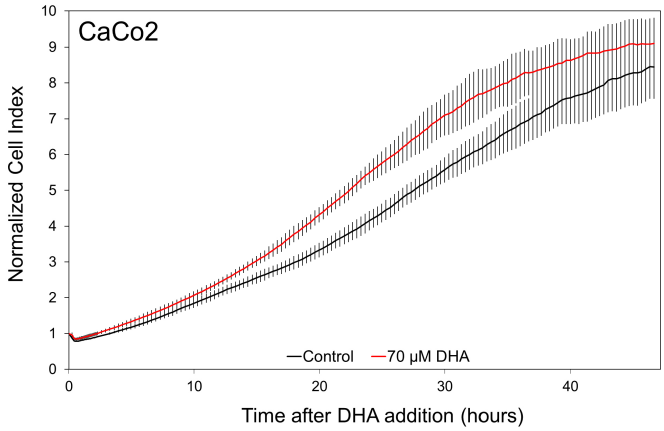
CaCo2
Normalized Cell Index
10
9
8
7
6
5
4
3
2
1
0
0
10
20
30
40
Time after DHA addition (hours)
Control
70 μM DHA

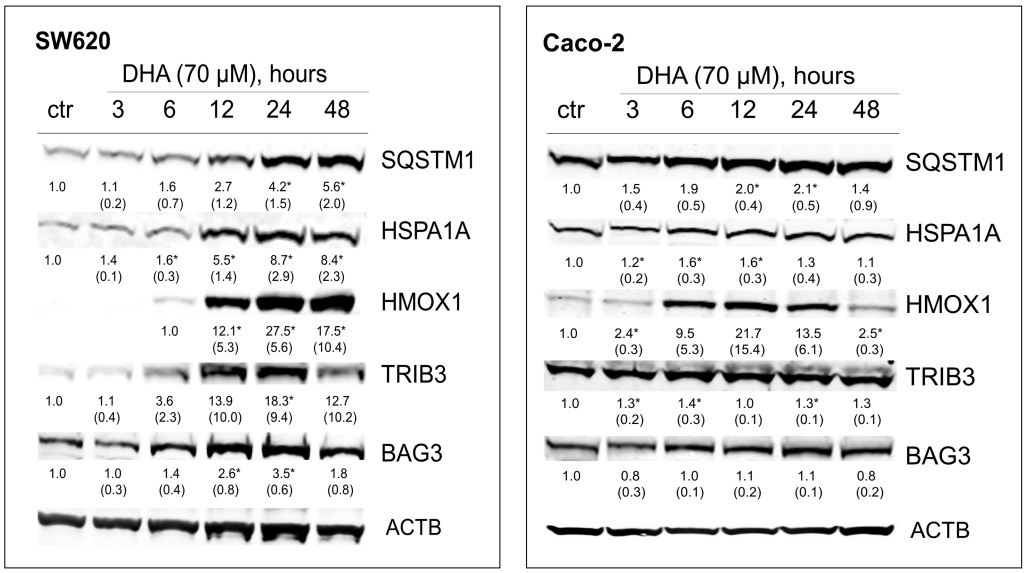
SW620
DHA (70 μM), hours
ctr 3 6 12 24 48
SQSTM1
1.0 1.1 (0.2) 1.6 (0.7) 2.7 (1.2) 4.2* (1.5) 5.6* (2.0)
HSPA1A
1.0 1.4 (0.1) 1.6* (0.3) 5.5* (1.4) 8.7* (2.9) 8.4* (2.3)
HMOX1
1.0 12.1* (5.3) 27.5* (5.6) 17.5* (10.4)
TRIB3
1.0 1.1 (0.4) 3.6 (2.3) 13.9 (10.0) 18.3* (9.4) 12.7 (10.2)
BAG3
1.0 1.0 (0.3) 1.4 (0.4) 2.6* (0.8) 3.5* (0.6) 1.8 (0.8)
ACTB
Caco-2
DHA (70 μM), hours
ctr 3 6 12 24 48
SQSTM1
1.0 1.5 (0.4) 1.9 (0.5) 2.0* (0.4) 2.1* (0.5) 1.4 (0.9)
HSPA1A
1.0 1.2* (0.2) 1.6* (0.3) 1.6* (0.3) 1.3 (0.4) 1.1 (0.3)
HMOX1
1.0 2.4* (0.3) 9.5 (5.3) 21.7 (15.4) 13.5 (6.1) 2.5* (0.3)
TRIB3
1.0 1.3* (0.2) 1.4* (0.3) 1.0 (0.1) 1.3* (0.1) 1.3 (0.1)
BAG3
1.0 0.8 (0.3) 1.0 (0.1) 1.1 (0.2) 1.1 (0.1) 0.8 (0.2)
ACTB

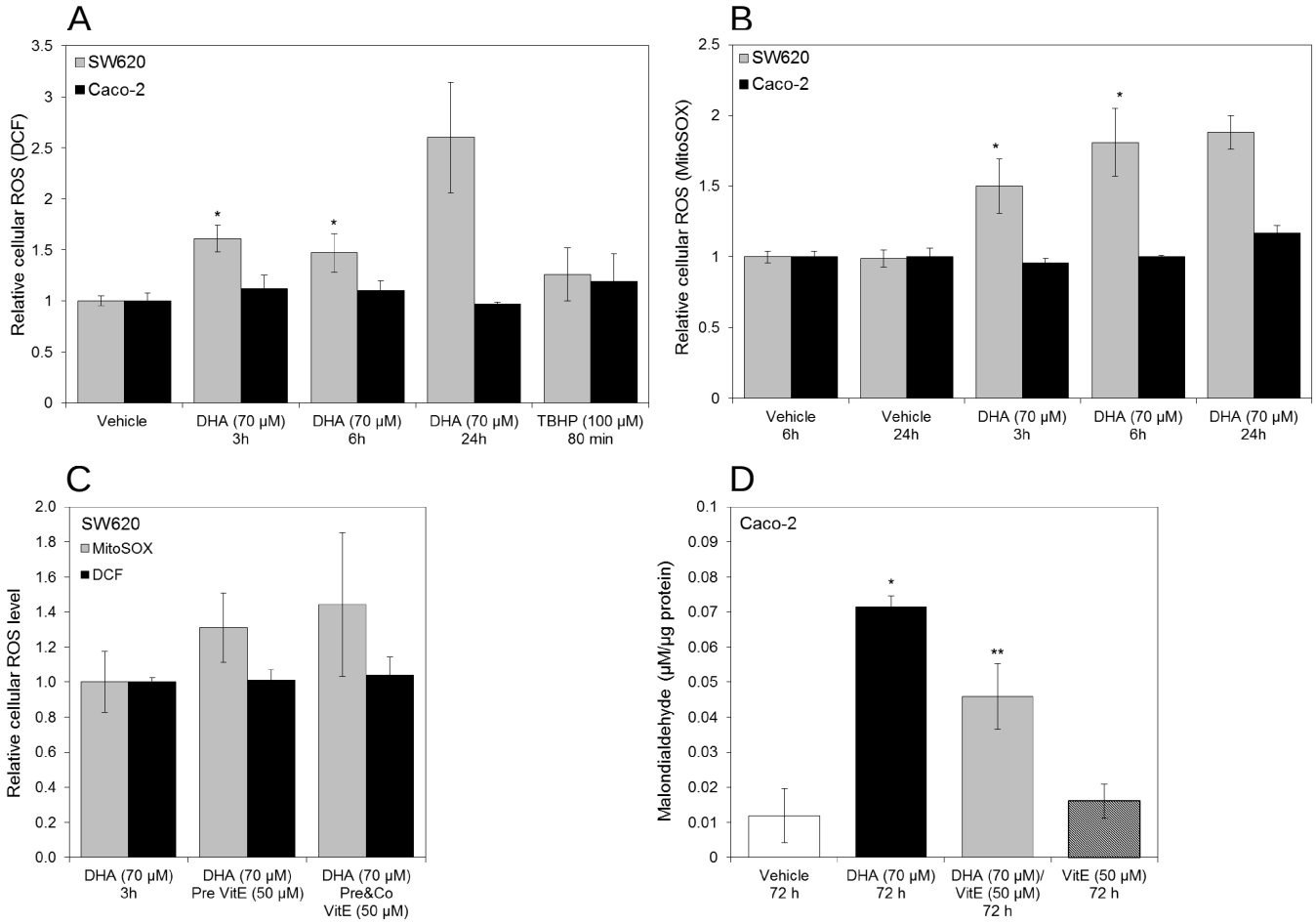
A
SW620
Caco-2
Relative cellular ROS (DCF)
Vehicle
DHA (70 µM) 3h
DHA (70 µM) 6h
DHA (70 µM) 24h
TBHP (100 µM) 80 min
B
SW620
Caco-2
Relative cellular ROS (MitoSOX)
Vehicle 6h
Vehicle 24h
DHA (70 µM) 3h
DHA (70 µM) 6h
DHA (70 µM) 24h
C
SW620
MitoSOX
DCF
Relative cellular ROS level
DHA (70 µM) 3h
DHA (70 µM) Pre VitE (50 µM)
DHA (70 µM) Pre&Co VitE (50 µM)
D
Caco-2
Malondialdehyde (µM/µg protein)
Vehicle 72 h
DHA (70 µM) 72 h
DHA (70 µM)/ VitE (50 µM) 72 h
VitE (50 µM) 72 h

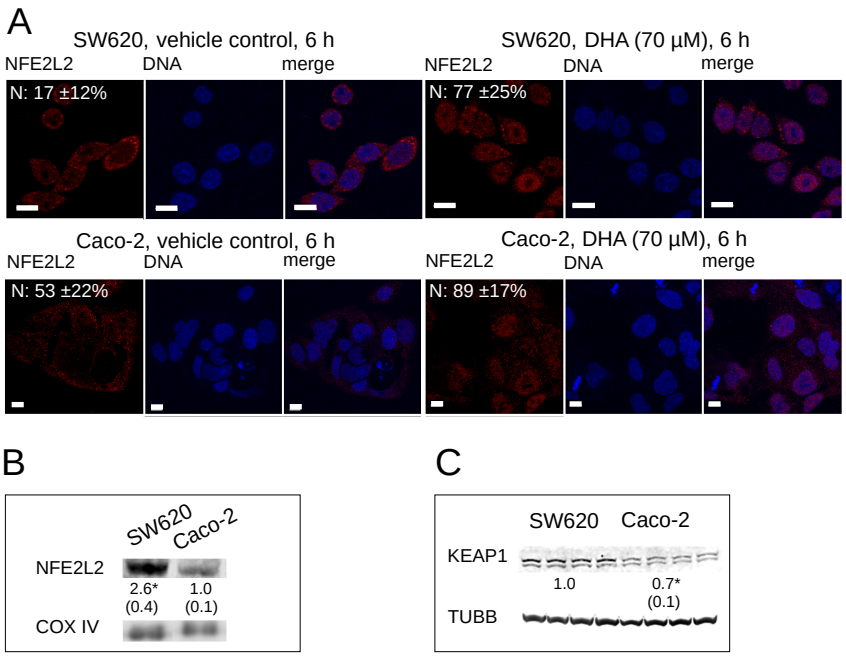
A
SW620, vehicle control, 6 h
NFE2L2
DNA
merge
N: 17 ±12%
SW620, DHA (70 µM), 6 h
NFE2L2
DNA
merge
N: 77 ±25%
Caco-2, vehicle control, 6 h
NFE2L2
DNA
merge
N: 53 ±22%
Caco-2, DHA (70 µM), 6 h
NFE2L2
DNA
merge
N: 89 ±17%

B
SW620
Caco-2
NFE2L2
2.6*
(0.4)
1.0
(0.1)
COX IV

C
SW620
Caco-2
KEAP1
1.0
0.7*
(0.1)
TUBB

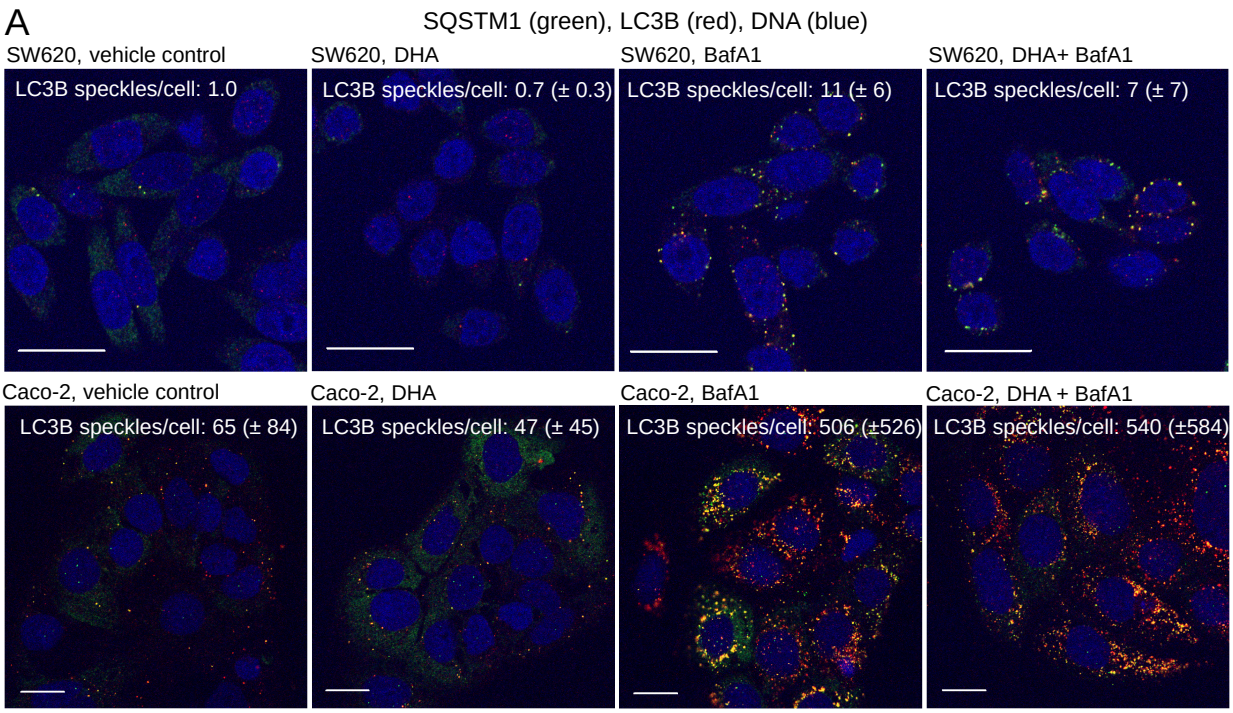
A
SQSTM1 (green), LC3B (red), DNA (blue)
SW620, vehicle control
LC3B speckles/cell: 1.0
SW620, DHA
LC3B speckles/cell: 0.7 (± 0.3)
SW620, BafA1
LC3B speckles/cell: 11 (± 6)
SW620, DHA+ BafA1
LC3B speckles/cell: 7 (± 7)
Caco-2, vehicle control
LC3B speckles/cell: 65 (± 84)
Caco-2, DHA
LC3B speckles/cell: 47 (± 45)
Caco-2, BafA1
LC3B speckles/cell: 506 (±526)
Caco-2, DHA + BafA1
LC3B speckles/cell: 540 (±584)

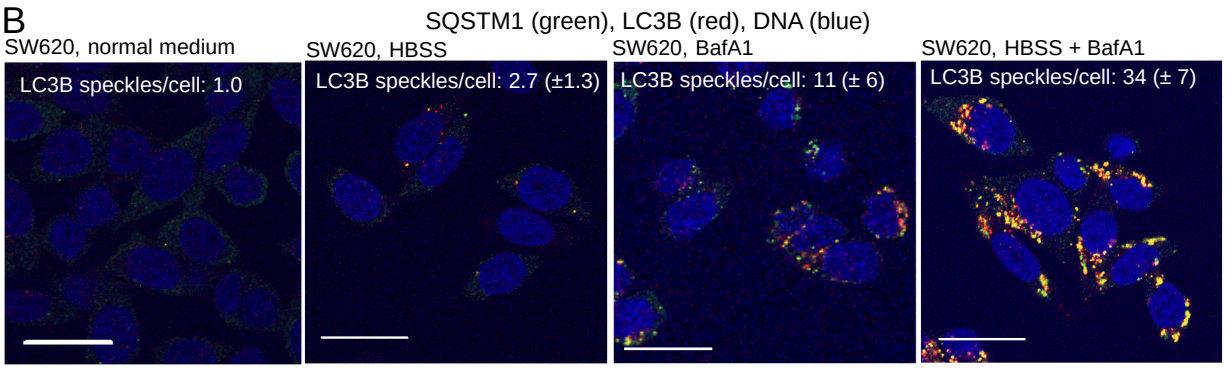
B
SQSTM1 (green), LC3B (red), DNA (blue)
SW620, normal medium
LC3B speckles/cell: 1.0
SW620, HBSS
LC3B speckles/cell: 2.7 (±1.3)
SW620, BafA1
LC3B speckles/cell: 11 (± 6)
SW620, HBSS + BafA1
LC3B speckles/cell: 34 (± 7)

C

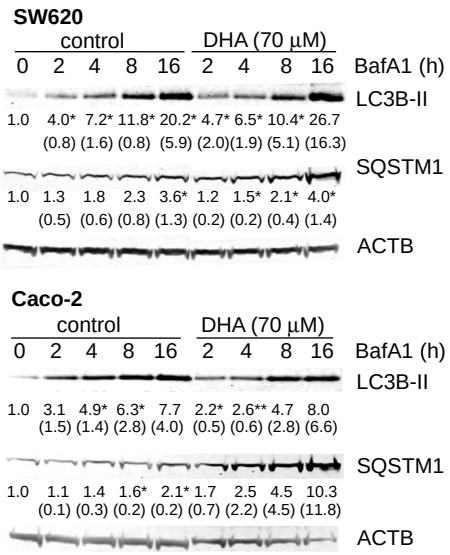
SW620
control
DHA (70 μM)
0 2 4 8 16 2 4 8 16 BafA1 (h)
LC3B-II
1.0 4.0* 7.2* 11.8* 20.2* 4.7* 6.5* 10.4* 26.7
(0.8) (1.6) (0.8) (5.9) (2.0)(1.9) (5.1) (16.3)
SQSTM1
1.0 1.3 1.8 2.3 3.6* 1.2 1.5* 2.1* 4.0*
(0.5) (0.6) (0.8) (1.3) (0.2) (0.2) (0.4) (1.4)
ACTB
Caco-2
control
DHA (70 μM)
0 2 4 8 16 2 4 8 16 BafA1 (h)
LC3B-II
1.0 3.1 4.9* 6.3* 7.7 2.2* 2.6** 4.7 8.0
(1.5) (1.4) (2.8) (4.0) (0.5) (0.6) (2.8) (6.6)
SQSTM1
1.0 1.1 1.4 1.6* 2.1* 1.7 2.5 4.5 10.3
(0.1) (0.3) (0.2) (0.2) (0.7) (2.2) (4.5) (11.8)
ACTB

D

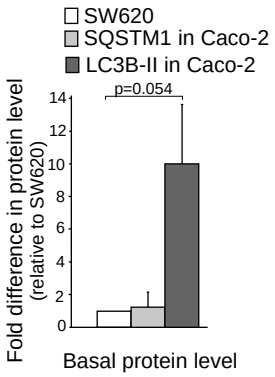
SW620
SQSTM1 in Caco-2
LC3B-II in Caco-2
p=0.054
Fold difference in protein level
(relative to SW620)
Basal protein level

E

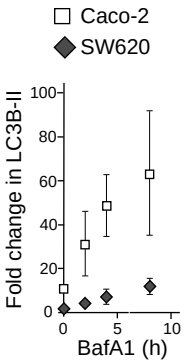
Caco-2
SW620
Fold change in LC3B-II
BafA1 (h)

F

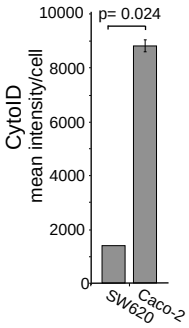
p= 0.024
CytoID
mean intensity/cell
SW620
Caco-2

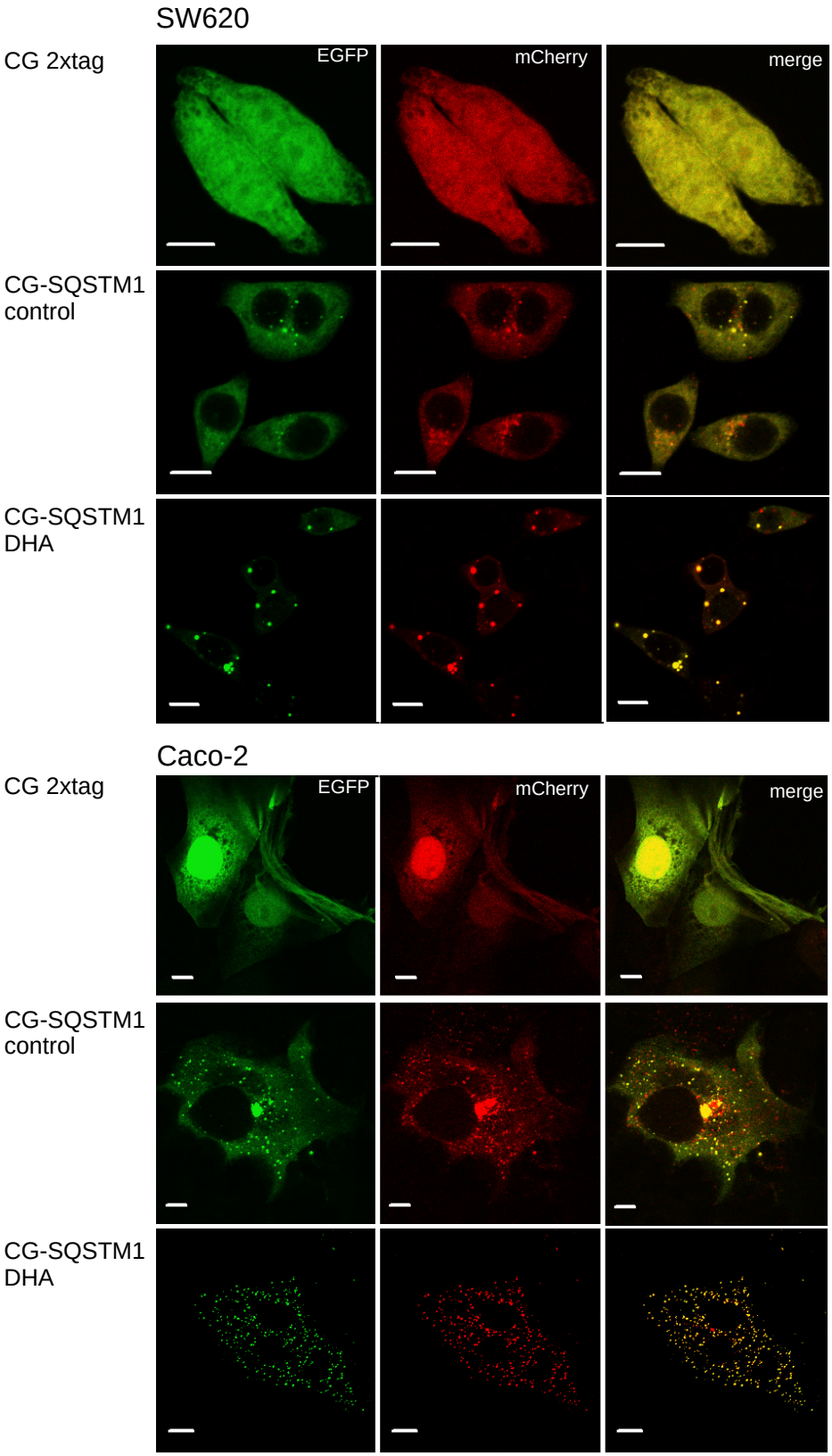
SW620
CG 2xtag
EGFP
mCherry
merge
CG-SQSTM1 control
CG-SQSTM1 DHA
Caco-2
CG 2xtag
EGFP
mCherry
merge
CG-SQSTM1 control
CG-SQSTM1 DHA

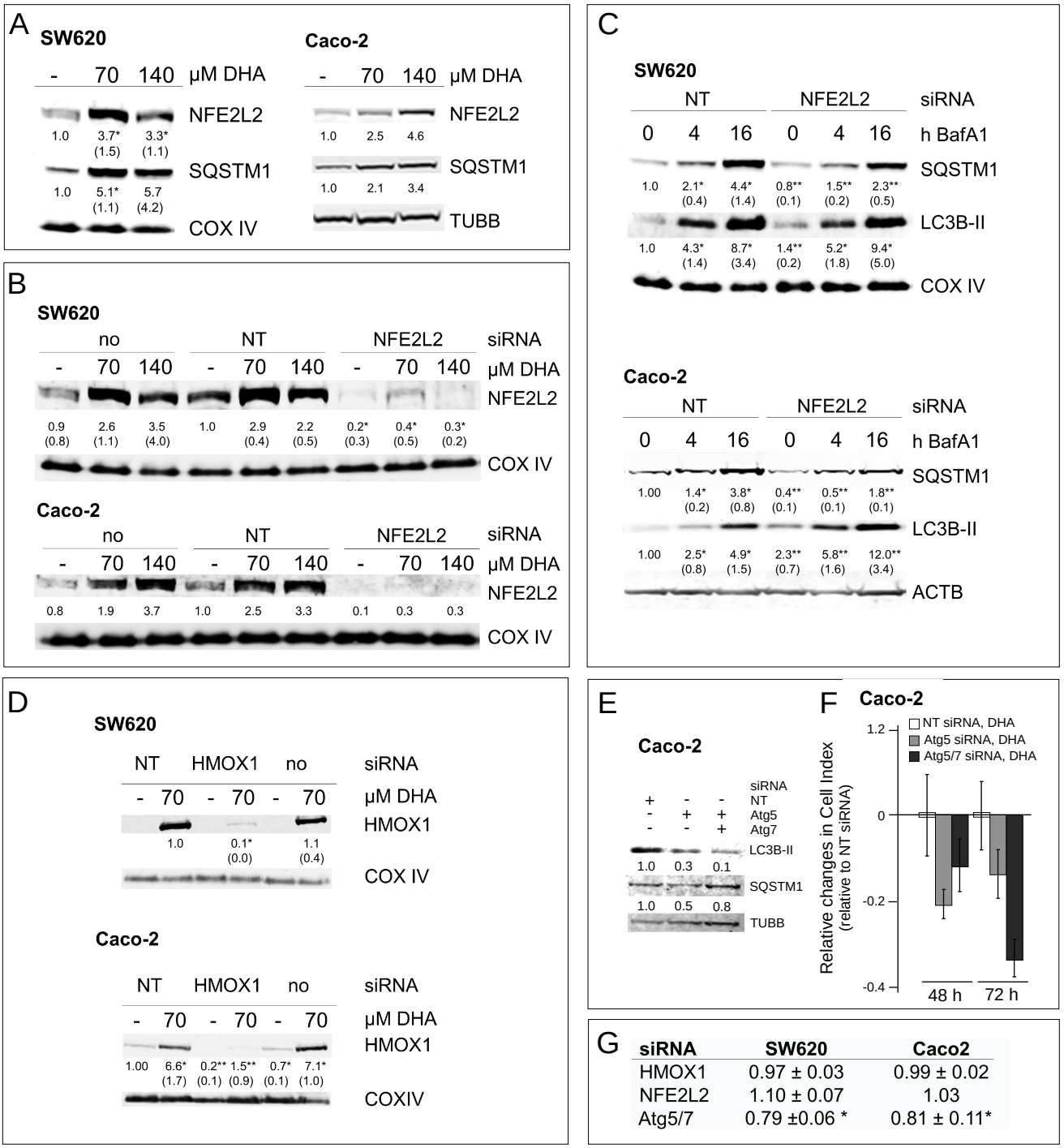

G

siRNA	SW620	Caco2
HMOX1	0.97 ± 0.03	0.99 ± 0.02
NFE2L2	1.10 ± 0.07	1.03
Atg5/7	0.79 ±0.06 *	0.81 ± 0.11*

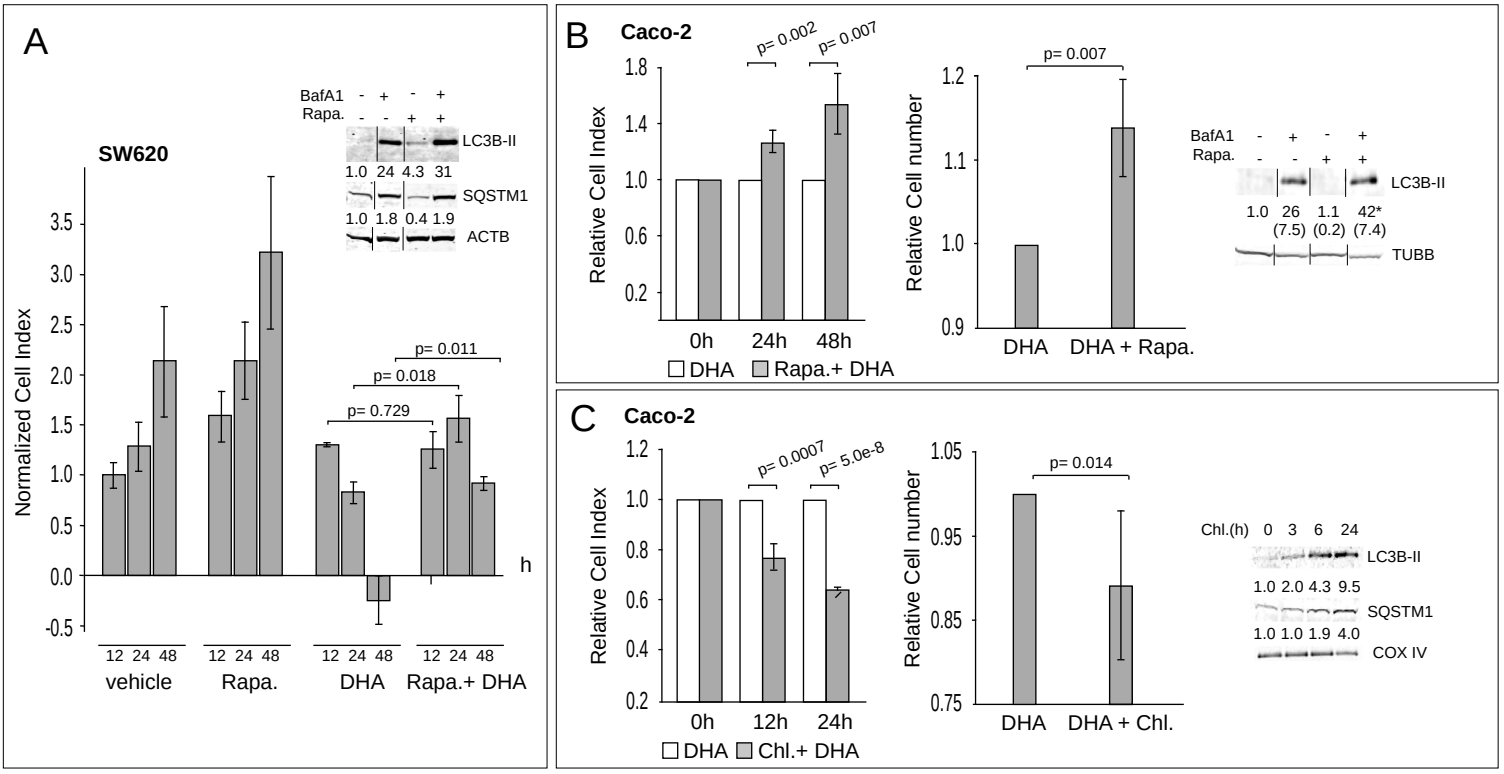
A
SW620
Normalized Cell Index
BafA1 - + - +
Rapa. - - + +
LC3B-II
1.0 24 4.3 31
SQSTM1
1.0 1.8 0.4 1.9
ACTB
p= 0.011
p= 0.018
p= 0.729
h
12 24 48
vehicle
Rapa.
DHA
Rapa.+ DHA
B
Caco-2
Relative Cell Index
p= 0.002
p= 0.007
0h 24h 48h
DHA
Rapa.+ DHA
Relative Cell number
p= 0.007
DHA
DHA + Rapa.
BafA1 - + - +
Rapa. - - + +
LC3B-II
1.0 26 1.1 42*
(7.5) (0.2) (7.4)
TUBB
C
Caco-2
Relative Cell Index
p= 0.0007
p= 5.0e-8
0h 12h 24h
DHA
Chl.+ DHA
Relative Cell number
p= 0.014
DHA
DHA + Chl.
Chl.(h) 0 3 6 24
LC3B-II
1.0 2.0 4.3 9.5
SQSTM1
1.0 1.0 1.9 4.0
COX IV